Supplementary Information

Highly stable self-assembled nanotubes from a bipyridinium-based amphiphilic pseudopeptide.

Alejandro Vila,[a] Valentina Gauci,[a] and Arturo Blanco-Gómez*[a]

[a] Interdisciplinary Center for Chemistry and Biology (CICA) and Department of Chemistry, Faculty of Science, University of Coruña, 15071 A Coruña, Spain.

email: arturo.blanco.gomez@udc.es

Table of contents:

S1. General methods and instrumentation.

All reagents and solvents were obtained from commercial sources and used as received, without additional purification. Compound **B**·I was synthesized following a previously reported procedure.[1] Milli-Q water was produced using a Millipore Gradient A10 system. Lyophilization, when required, was performed with a Telstar Cryodos -80 freeze-dryer. NMR spectra were recorder on a Bruker ADVANCE 500 equipped with dual $^{1}H/^{13}C$ cryoprobe and operating at 500 and 126 MHz for ^{1}H and ^{13}C, respectively, or on a Bruker ADVANCE III HD 400 equipped with BBFO probe for broadband observation and operating at 400 and 101 MHz for ^{1}H and ^{13}C, respectively. The NMR solvents used were deuterated water (D_2O), and dimethylsulfoxide-d6 (DMSO-d6). Chemical shifts are reported in ppm relative tetramethylsilane (TMS, δ = 0 ppm) or, otherwise, to the residual internal non deuterated solvent signal (D_2O, δ = 4.79 ppm, DMSO-d6, δ = 2.50 ppm). High-resolution mass spectrometry (HRMS) experiments were carried out in an ESI-TOF LTQ-Orbitrap Discovery mass spectrometer. pH was measured using a Fisherbrand accumet AE150 pHmeter microsamples with Ag/AgCl reference element. Dynamic oscillatory rheology measurements were conducted using a Discovery DHR2 rheometer (TA Instruments-Waters LLC), employing parallel steel plate geometry (25 mm) and Peltier cooling (25 °C). Transmission electron microscopy (TEM) images were acquired using a Jeol JEM-1010 electron microscope operating at 100 kV and equipped with a Megaview II camera. IR spectra were recorded on a Bruker Vector 22 FTIR spectrometer equipped with GoldenGate KRS-5 optics (Specac). Circular dichroism (CD) spectra were acquired using a Jasco J-815 150S spectropolarimeter with a coupled PTC-423S/15 Peltier Thermostatted Single Cell Holder (water cooler). UV-Vis spectra measurements were recorded on a Jasco V-650 spectrometer. Steady-state emission measurements were performed with an Agilent Cary Eclipse Fluorescence Spectrophotometer, equipped with a Peltier temperature control system (water cooled).

[1] A. Blanco-Gómez, A., I. Neira, J. L. Barriada, M. Melle-Franco, C. Peinador, M. D. García, *Chem. Sci.*, 2019, **10**, 10680.

S2. Synthesis and characterization data of precursor A·Br.

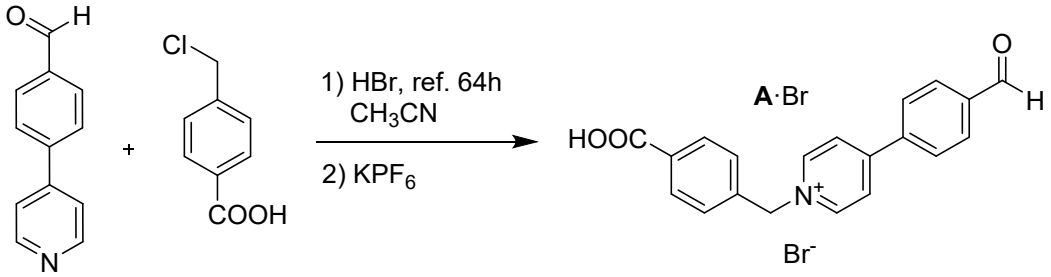

A mixture of 4-(4-pyridyl)benzaldehyde (0.90 g, 4.98 mmol, 1.2 equiv.) and 4-(chloromethyl)benzoic acid (0.71 g, 4.15 mmol, 1 equiv.) in CH_3CN (50 mL) was stirred under reflux in a hot plate stirrer until complete dissolution. HBr (0.23 mL) was then added dropwise and the solution was stirred under reflux 64 h. The resulting precipitate was hot-filtered, washed with hot CH_3CN (3 x 10 mL), Et_2O (3 × 10 mL) and dried under vacuum to yield **A**·Br as a white solid (1.32 g, 80%).

^{1}H NMR (400 MHz, D_2O) δ (ppm): 10.08 (s, 1H), 9.01 (d, J = 7.0 Hz, 1H), 8.43 (d, J = 6.9 Hz, 1H), 8.23 – 8.06 (m, 6H), 7.61 (d, J = 8.3 Hz, 2H), 5.96 (s, 2H).

^{13}C NMR (101 MHz, D_2O) δ (ppm) 195.6 (HC=O), 170.3 (COOH), 156.0 (C_{Py}), 144.7(CH_{Py}), 139.7 (C_{Ph}), 137.8 (C_{Ph}), 137.7 (C_{Ph}), 131.6 (C_{Ph}), 130.8 (CH_{Ph}), 130.6 (CH_{Ph}), 128.9 (CH_{Ph}), 128.9 (CH_{Ph}), 126.1 (CH_{Py}), 63.4 (CH_2).

HRMS (ESI) m/z: Calcd for $C_{20}H_{16}NO_3^+$ 318.1125, found 318.1126; Calcd for $C_{21}H_{20}NO_4^+$ 350.1387, found 350.1389.

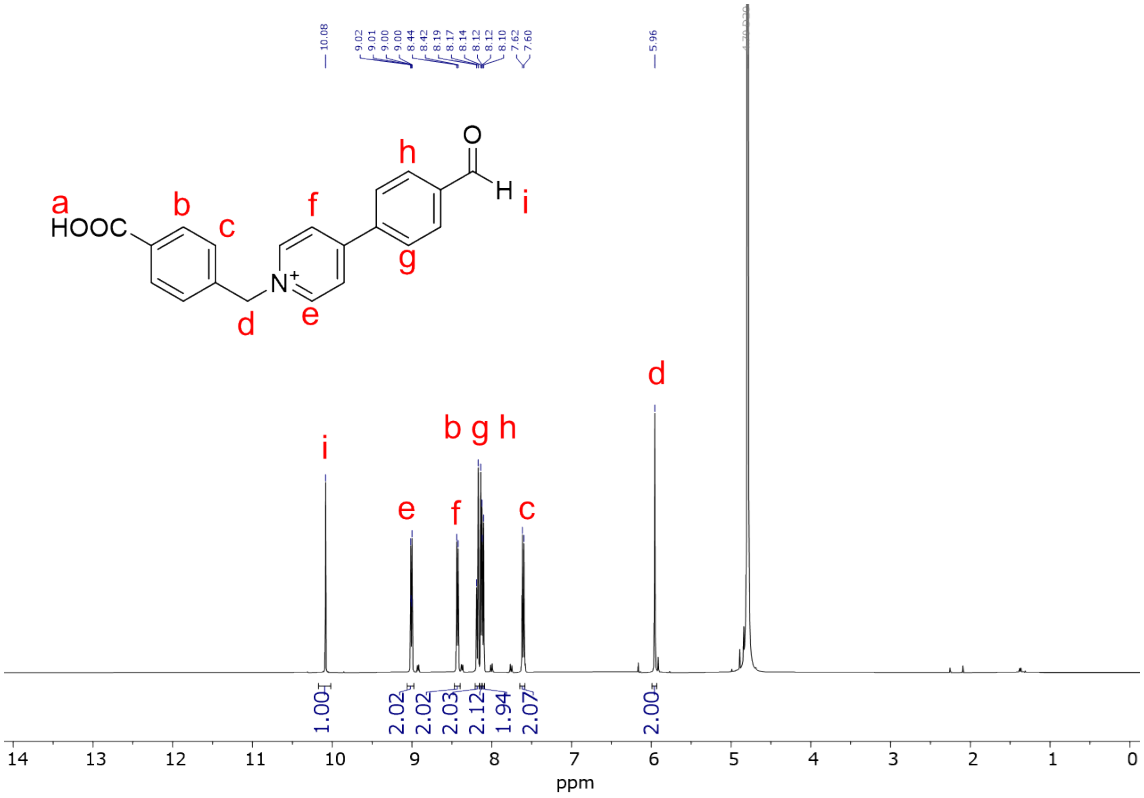

Fig. S1 ^{1}H NMR (400 MHz, D_2O) spectrum of **A**·Br.

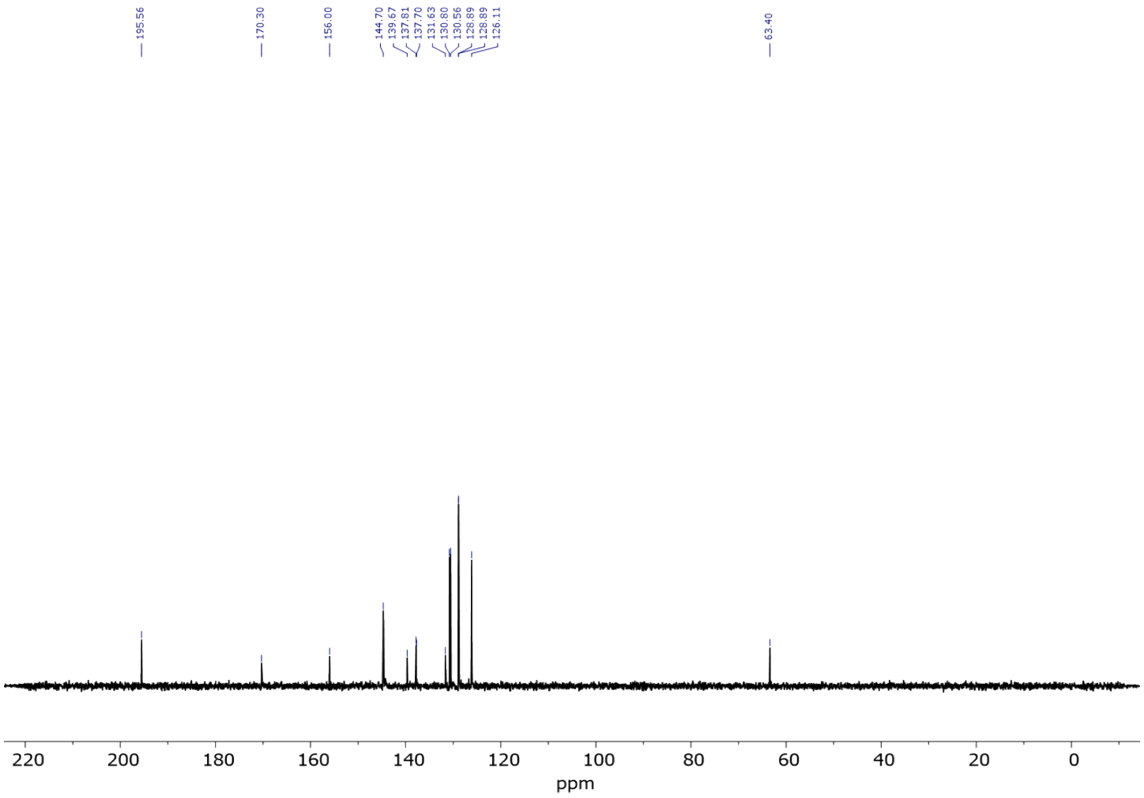

Fig. S2 $^{13}C\{^{1}H\}$ NMR (101 MHz, D_2O) spectrum of **A**·Br.

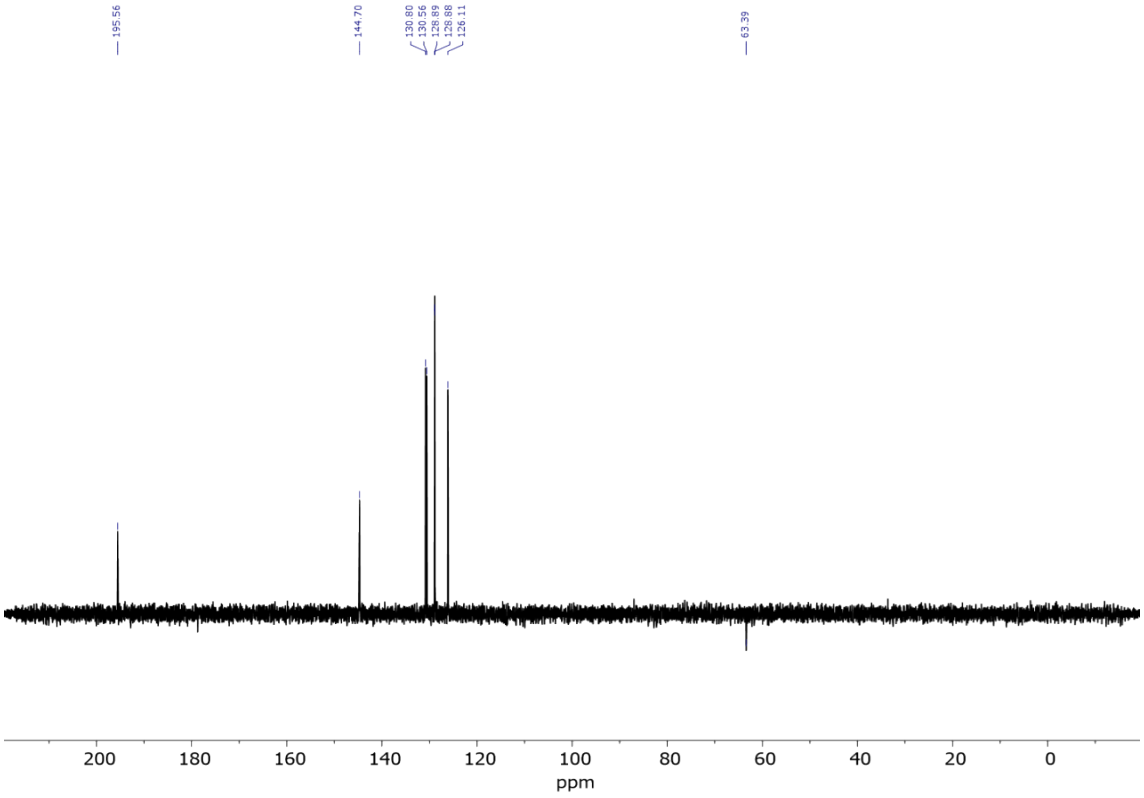

Fig. S3 DEPT-135 NMR (101 MHz, D_2O) spectrum of **A**·Br.

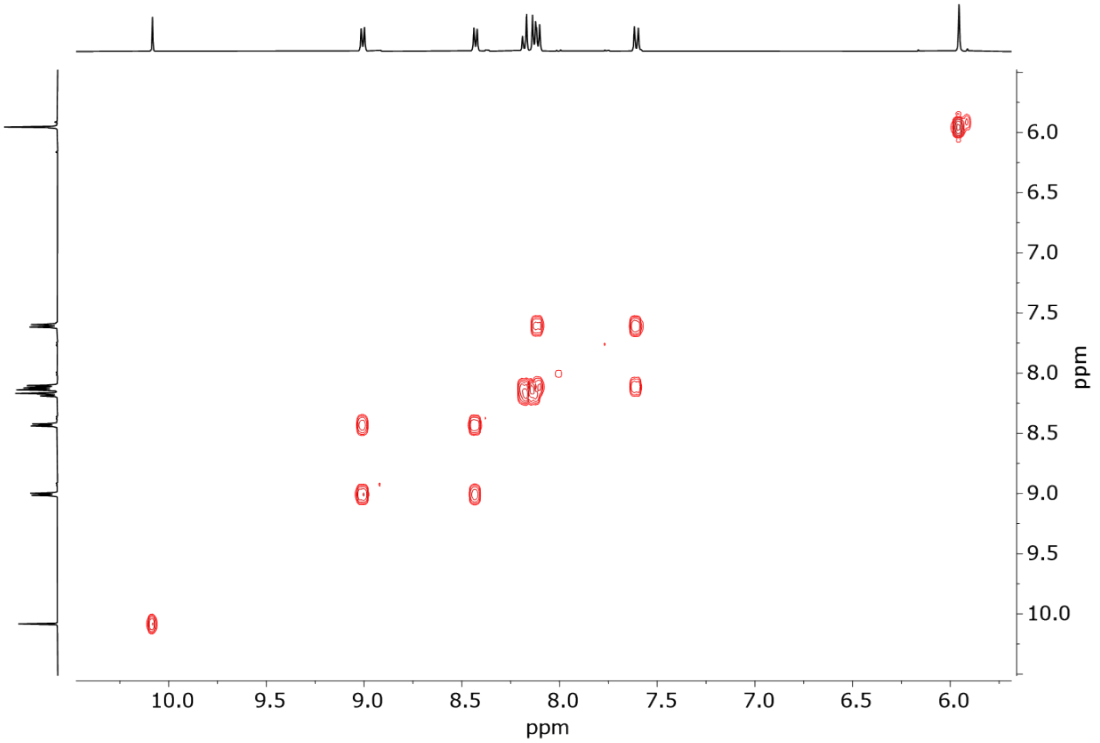

Fig. S4 ^{1}H-^{1}H COSY (400 MHz, D_2O) spectrum of **A**·Br.

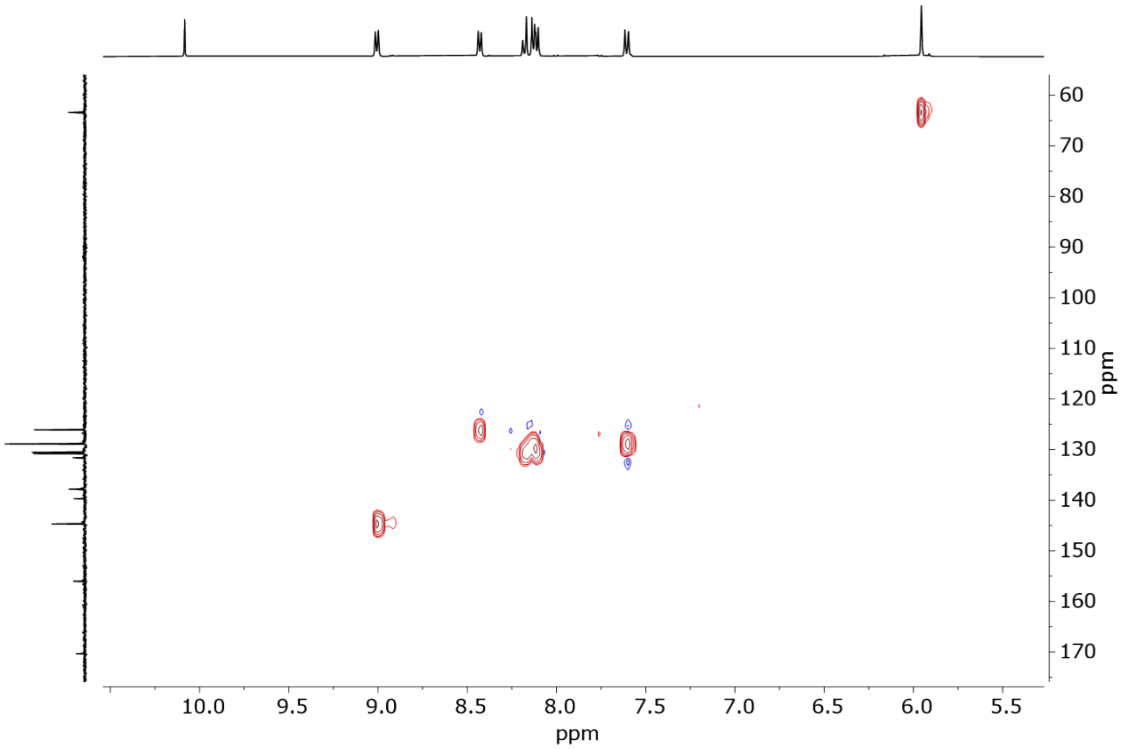

Fig. S5 ^{1}H-^{13}C HSQC (400 MHz, D_2O) spectrum of **A**·Br.

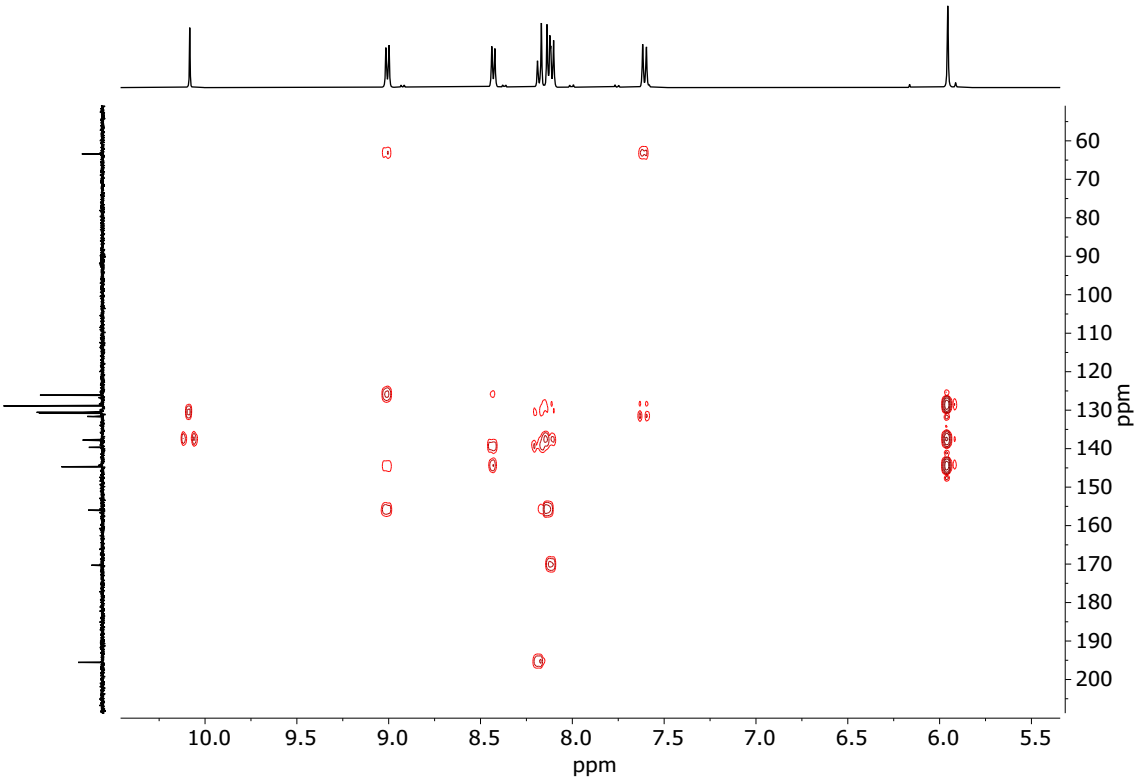

Fig. S6 ^{1}H-^{13}C HMBC (400 MHz, D_2O) spectrum of **A**·Br.

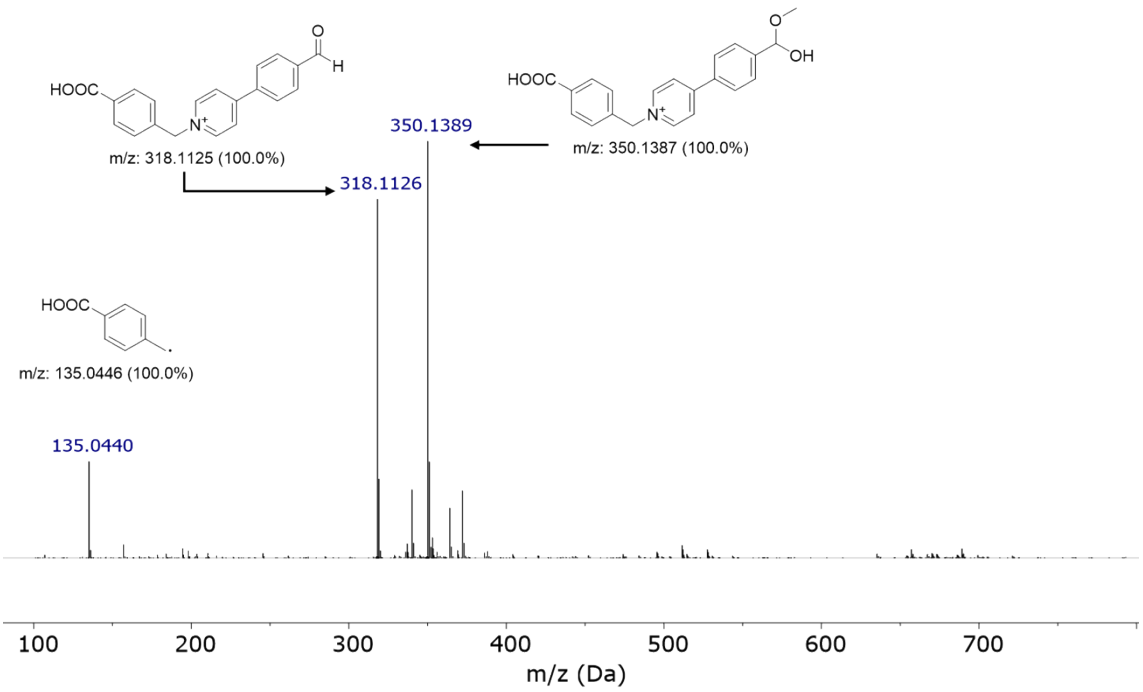

Fig. S7 HRMS-ESI spectrum of **A**·Br.

S3. Synthesis and characterization data of precursor C·2PF$_6$.

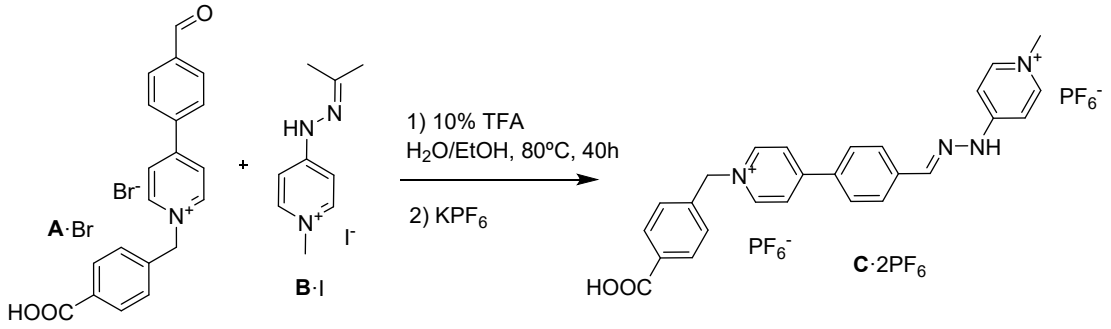

A mixture of **A**·Br (1.32 g, 3.3 mmol, 1.0 equiv.) and **B**·I (0.97 g, 3.3 mmol, 1.0 equiv.) in H_2O (125 mL) and EtOH (75 mL) was stirred at 80 °C in a hot plate stirrer until complete dissolution. TFA (25.5 µL, 0.33 mmol, 0.1 equiv.) was then added, and the reaction mixture was stirred at the same temperature for 40 h. Subsequently, KPF_6 (2.4 g, 13.2 mmol, 4.0 equiv.) was added and, after 30 min, the precipitate formed was collected by filtration, washed with H_2O (3 x 10 mL) and Et_2O (3 × 10 mL), and dried under vacuum to yield **C**·2PF$_6$ as a yellow solid (2.24 g, 95%).

^{1}H NMR (500 MHz, DMSO-d6) δ (ppm): 9.22 (d, *J* = 6.5 Hz, 2H), 8.60 (d, *J* = 6.5 Hz, 2H), 8.35 (s, 1H), 8.16 (d, *J* = 8.1 Hz, 3H), 8.09 (d, *J* = 6.9 Hz, 1H), 8.05 (d, *J* = 8.3 Hz, 2H), 7.99 (d, *J* = 8.0 Hz, 2H), 7.60 (d, *J* = 8.0 Hz, 3H), 6.94 (d, *J* = 7.2 Hz, 1H), 5.91 (s, 2H), 3.90 (s, 3H).

^{13}C NMR (126 MHz, DMSO-d6) δ (ppm): 167.2 (COOH), 155.4 (C_{Py}) 154.3 (C_{Py}), 146.2 (C=N), 145.0 (CH_{Py}), 143.6 (CH_{Py}), 142.9 (CH_{Py}), 138.1 (C_{Ph}), 138,0 (C_{Ph}) 134.2 (C_{Ph}), 130.0 (CH_{Ph}), 128.8 (CH_{Ph}), 128.4 (CH_{Ph}), 128.1 (CH_{Ph}), 124.9 (CH_{Py}), 109.8 (CH_{Py}), 107.1 (CH_{Py}), 62.1 (CH_2), 44.3 (CH_3).

HRMS (ESI) m/z: Calcd for $C_{26}H_{23}N_4O_2^+$ 423,1816; Found 423.1815; Calcd for $C_{26}H_{24}N_4O_2^{2+}$ 212.0944; Found 212.0944; Calcd for $C_{18}H_{17}N_4^+$ 289.1448, Found 289.1449; Calcd for C8H7O2$^\bullet$ 135.0446; Found 135.0440.

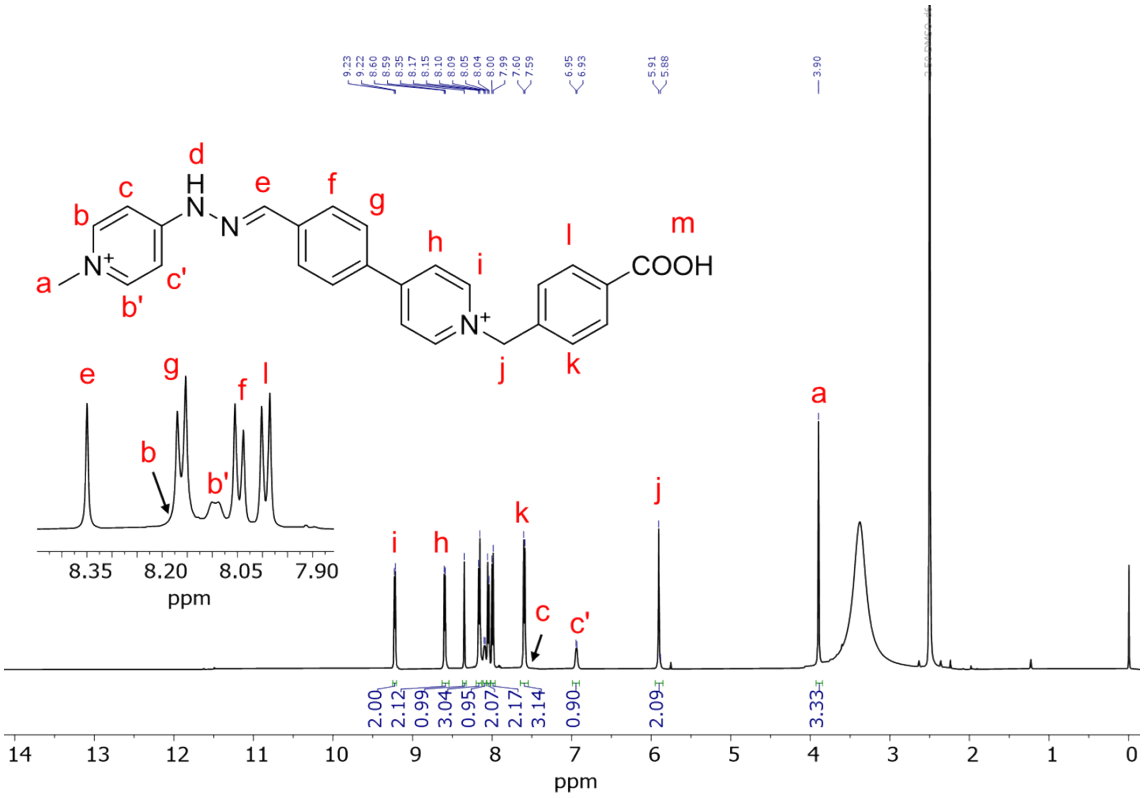

Fig. S8 ^{1}H NMR (500 MHz, DMSO-d6) spectrum of **C**·2PF$_6$. *Inset*: Scaling up of the 7.9-8.4 ppm range of the ^{1}H-NMR spectrum.

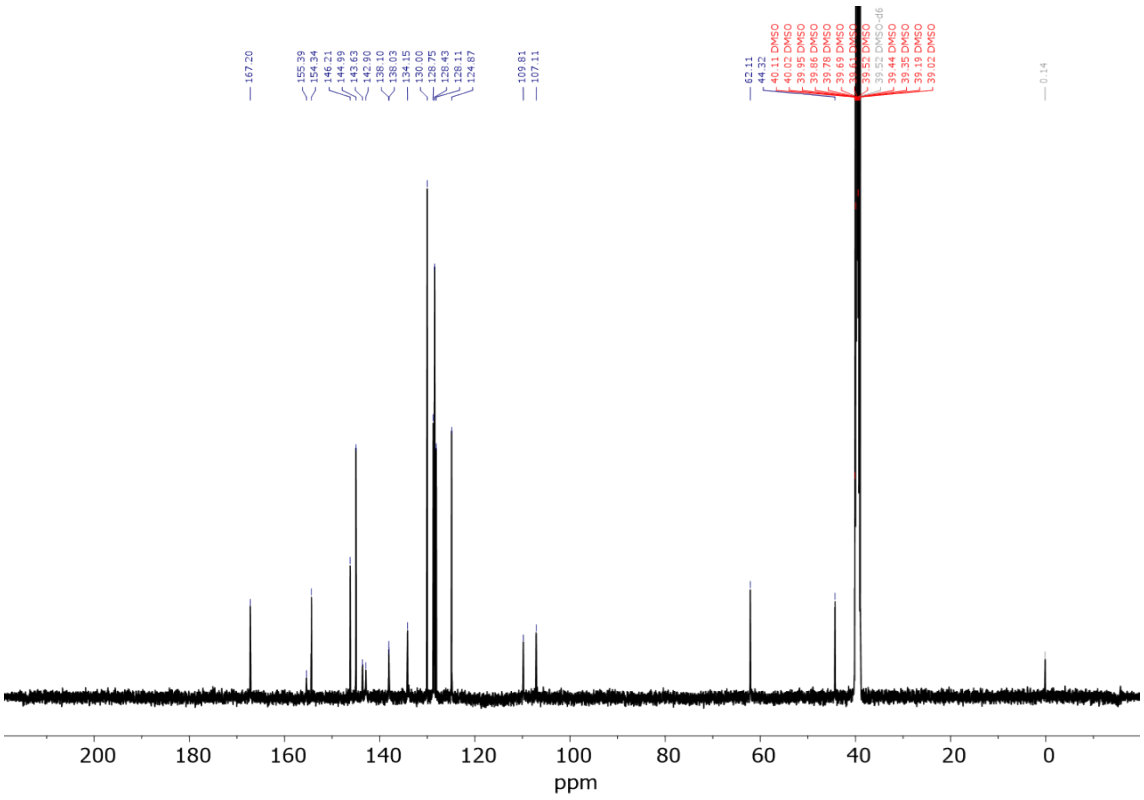

Fig. S9 ^{13}C{^{1}H} NMR (126 MHz, DMSO-d6) spectrum of **C**·2PF$_6$.

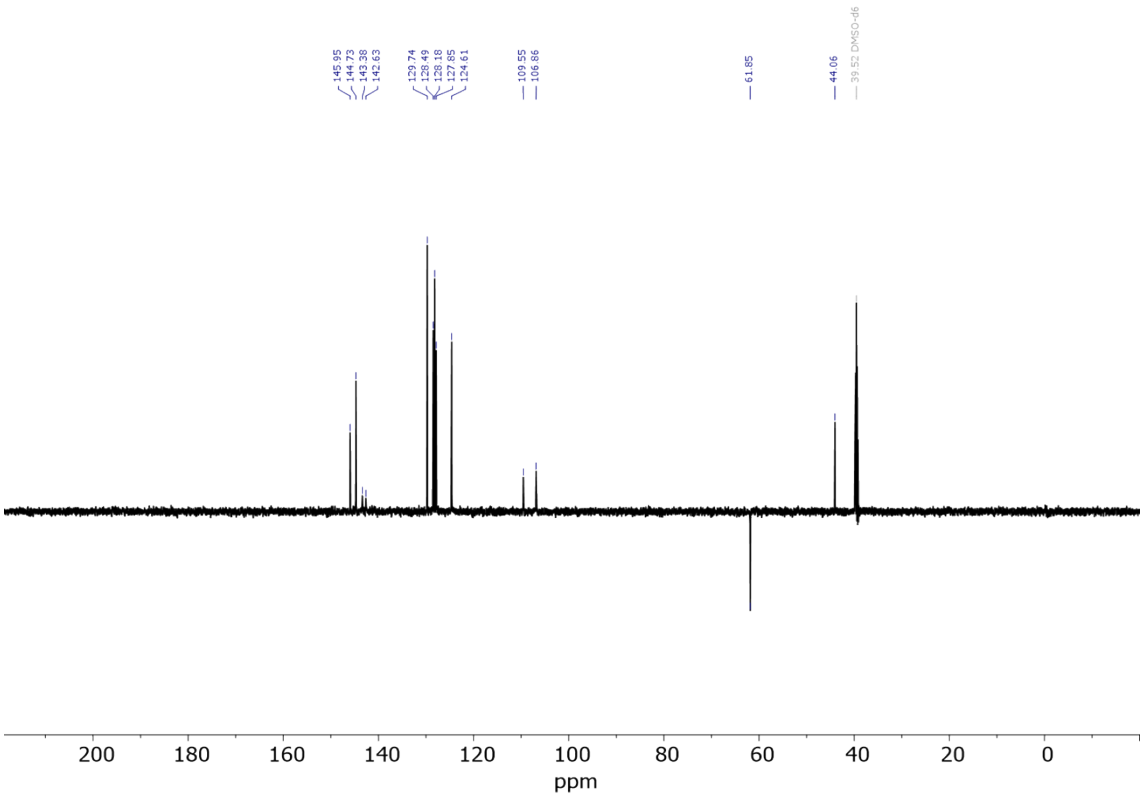

Fig. S10 DEPT-135 NMR (126 MHz, DMSO-d6) spectrum of **C**·2PF_6.

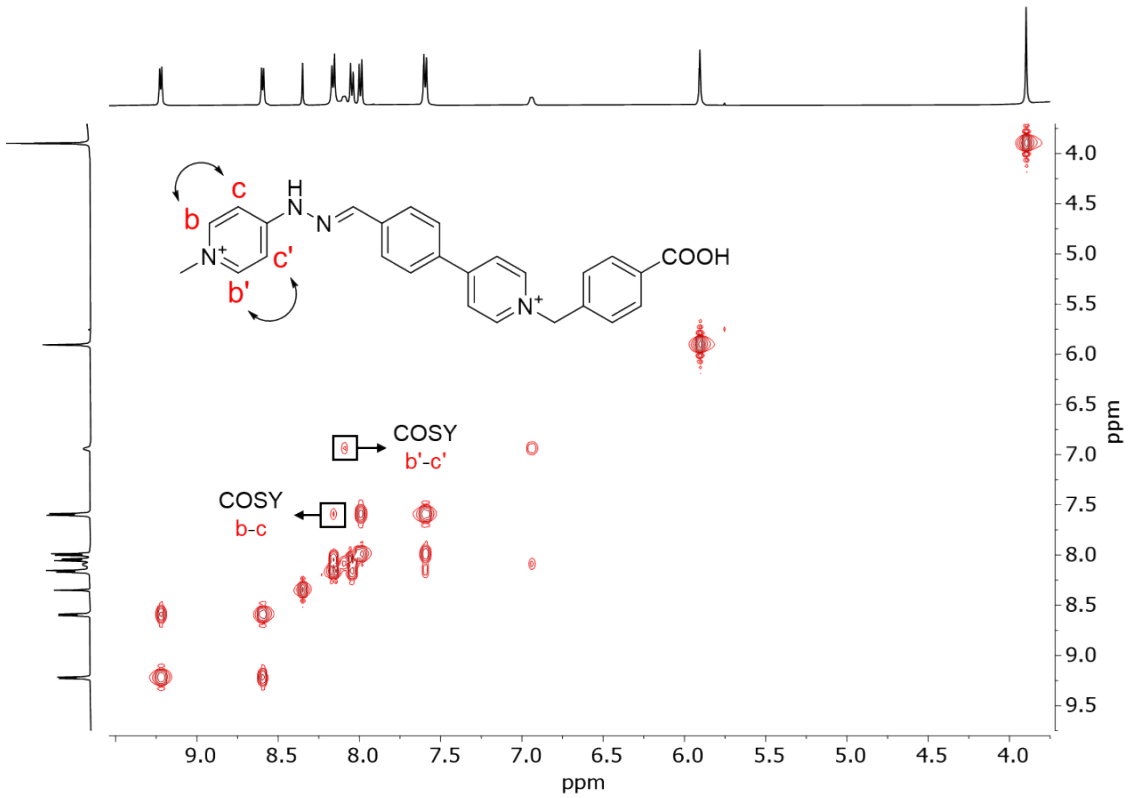

Fig. S11 ^{1}H-^{1}H COSY (500 MHz, DMSO-d6) spectrum of **C**·2PF_6.

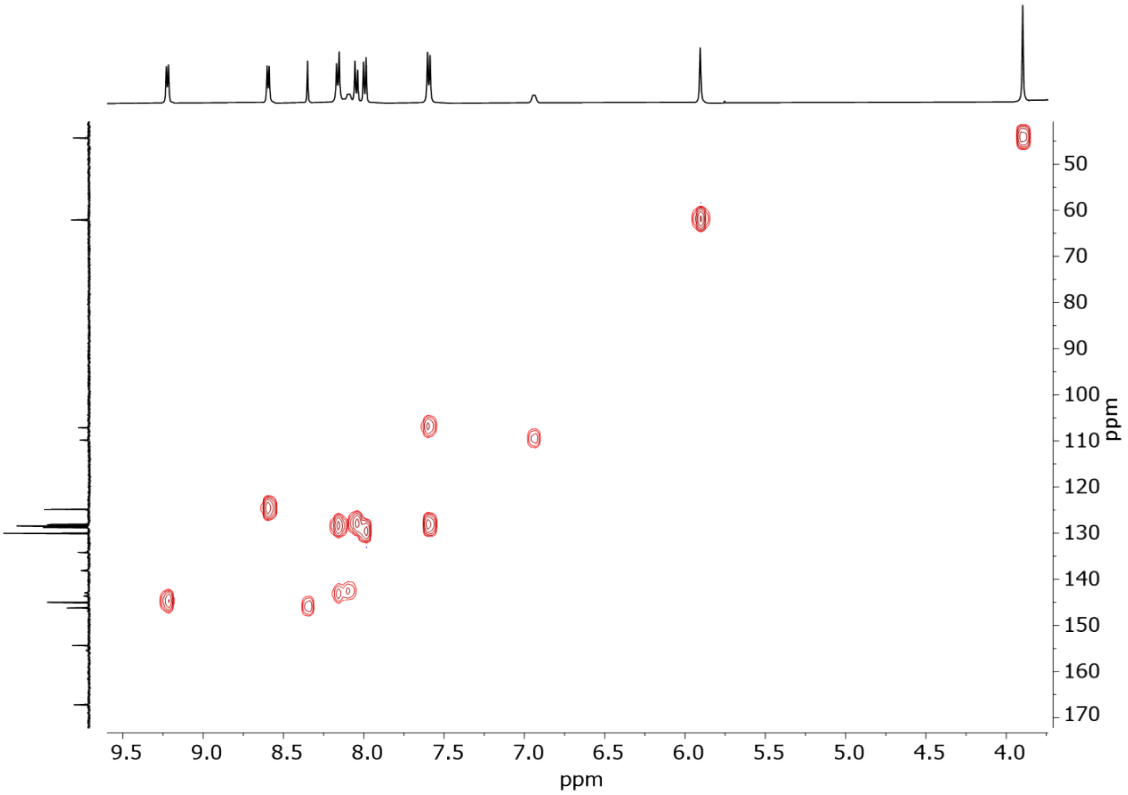

Fig. S12 ^{1}H-^{13}C HSQC (500 and 126 MHz, DMSO-d6) spectrum of **C**·2PF_6.

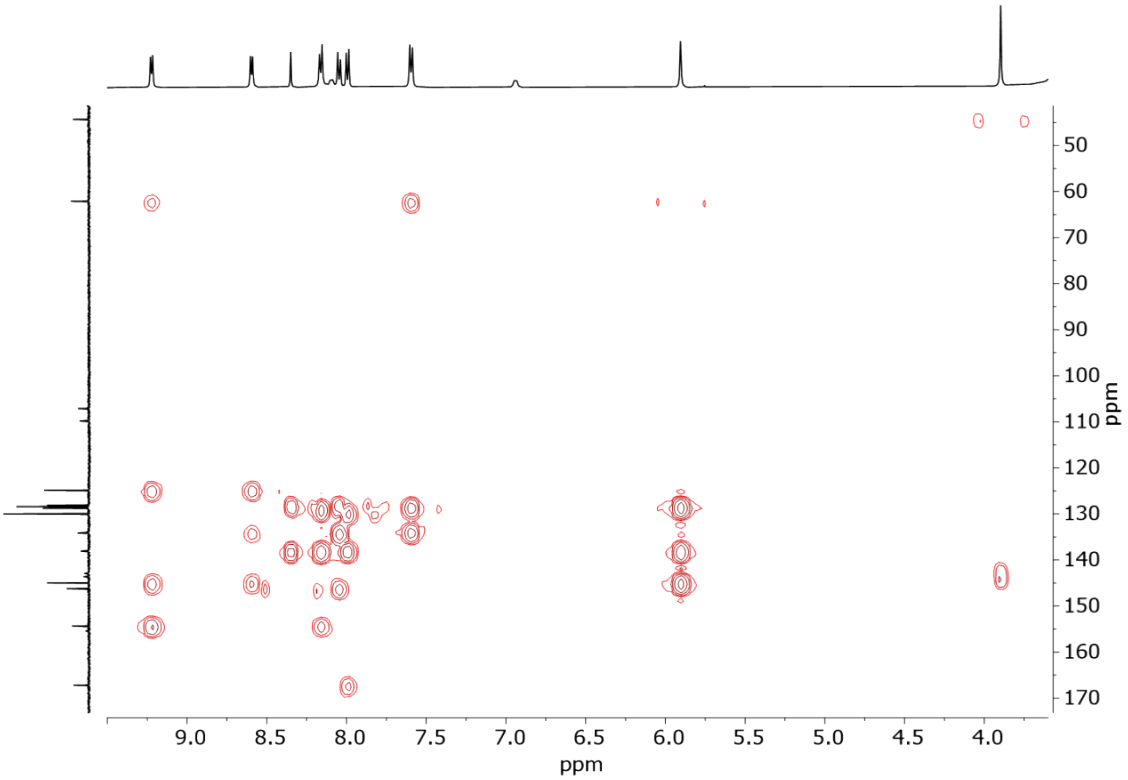

Fig. S13 ^{1}H-^{13}C HMBC (500 and 126 MHz, DMSO-d6) spectrum of **C**·2PF_6.

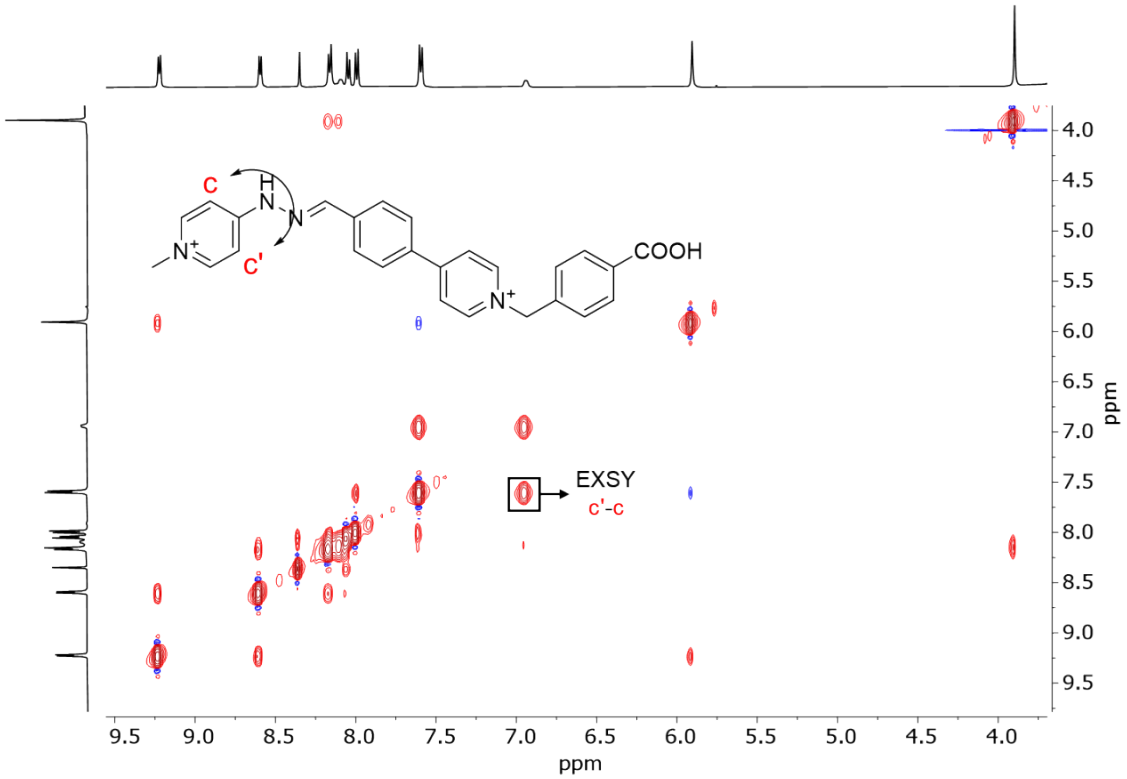

Fig. S14 ^{1}H-^{1}H NOESY (500 MHz, DMSO-d6) spectrum of **C**·2PF$_6$.

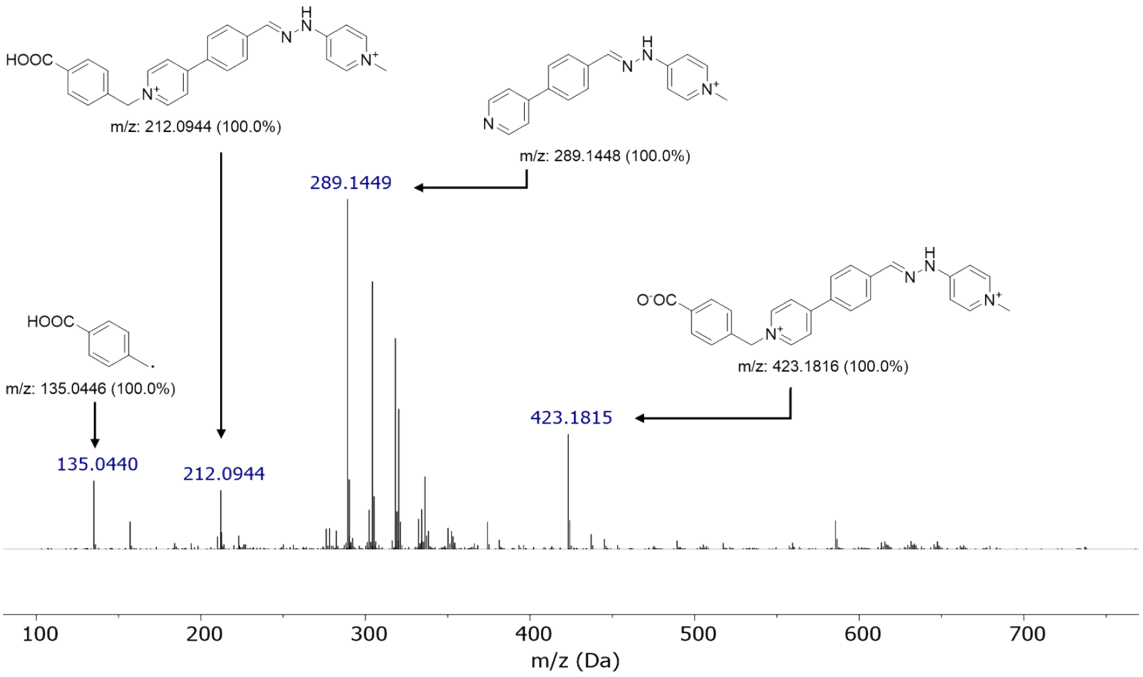

Fig. S15 HRMS-ESI spectrum of **C**·2PF$_6$.

S4. Synthesis and characterization data of 2.

2 was synthesized following Fmoc-based SPPS with Oxyma-B activation. All couplings and deprotection were monitored using the TNBS colorimetric test. 2-Chlorotrityl Chloride resin (0.3 g, 0.4 mmol, 1 equiv.) was swollen in 4 mL of dichloromethane (DCM) for 30 min. 0.03 mL of $SOCl_2$ was added, and the mixture was stirred for 2 hours. The resin was washed with DCM (3 x 5 mL) and dimethylformamide (DMF, 3 x 5 mL). A solution of Fmoc-L-Phe-OH (620 mg, 1.6 mmol, 4 equiv.) and DIPEA conc. (0.27 mL, 1.6 mmol, 4 equiv.) in 4 mL of DMF was added to the resin and stirred overnight. After that, 0.15 mL of MeOH was added, stirred for 20 min, and washed with DCM (3 x 5 mL) and DMF (3 x 5 mL). For the deprotection, a 20% piperidine in DMF was added (2 x 10 min, 5 mL) followed by washing with DCM (3 x 5 mL) and DMF (3 x 5 mL). For the second coupling, a solution of Fmoc-D-Phe-OH (620 mg, 1.6 mmol, 4 equiv.), Oxyma-B (296 mg, 1.6 mmol, 4 equiv.), and N,N'-Diisopropylcarbodiimide (DIC, 0.25 mL, 1.6 mmol, 4 equiv.) in 4 mL of DMF was prepared, added to the resin, and stirred for 1.5 hours. The resin was washed and deprotected as mentioned in the previous step. A new coupling with Fmoc-L-Phe-OH and subsequent deprotection were carried out using the same steps described above. For the final coupling, a solution of **C**·$2PF_6$ (1142 mg, 1.6 mmol, 4 equiv.), Oxyma-B (296 mg, 1.6 mmol, 4 equiv.), and DIC (0.25 mL, 1.6 mmol, 4 equiv.) in 4 mL of DMF was prepared, added to the resin, and stirred for 4 hours. After washing the resin with DCM and DMF, the pseudopeptide was cleaved from the resin by adding 5 mL of a solution of TFA, DCM, H_2O, and TIPS (49:49:1:1). After 2 hours of stirring, the cleavage solution was concentrated under air stream to obtain a sticky yellow solid. The solid were purified using HPLC (Agilent 1260 Infinity II) with a C-18 preparative HPLC column (ZORBAX®, 5 µm, 95 Å, 250 × 21.2 mm, Agilent InfinityLab) and a gradient of acetonitrile (MeCN)/water with 0.05% TFA as follows: t = 0–5 min, 25% MeCN; t = 30 min, 95% MeCN; t = 30–35 min, 95% MeCN (Rt = 15–16 min **2**).

^{1}H NMR (500 MHz, DMSO-d6) δ (ppm): 13.04 (s, 1H), 12.86 (s, 1H), 9.25 (d, *J* = 6.7 Hz, 2H), 8.60 (d, *J* = 6.6 Hz, 2H), 8.54 (t, *J* = 9.2 Hz, 2H), 8.44 (d, *J* = 7.4 Hz, 1H), 8.42 (s, 1H), 8.39 (d, *J* = 8.8 Hz, 1H), 8.36 (d, *J* = 7.3 Hz, 1H), 8.17 (d, *J* = 8.4 Hz, 2H), 8.08 (d, *J* = 8.3 Hz, 2H), 7.81 (d, *J* = 8.2 Hz, 2H), 7.74 (dd, *J* = 7.3, 2.7 Hz, 2H), 7.59 (d, *J* = 8.1 Hz, 2H), 7.31 – 7.14 (m, 10H), 7.14 – 7.04 (m, 6H), 5.89 (s, 2H), 4.71 – 4.57 (m, 2H), 4.49 (ddd, *J* = 10.2, 8.4, 4.5 Hz, 1H), 4.02 (s, 3H), 3.13 (dd, *J* = 13.7, 4.5 Hz, 1H), 2.85 (dd, *J* = 13.7, 10.2 Hz, 1H), 2.79 – 2.56 (m, 4H).

^{13}C NMR (126 MHz, DMSO-d6) δ (ppm): 172.8 (CO_2H), 170.9 (C=O), 170.8 (C=O), 165.2 (C=O), 154.2 (C_{Py}), 153.6 (C_{Py}), 145.9 (C=N), 145.0 (CH_{Py}), 144.9 (CH_{Py}), 144.1 (CH_{Py}), 138.3 (C_{Ph}), 137.6 (C_{Ph}), 137.5 (C_{Ph}), 137.4 (C_{Ph}), 137.1 (C_{Ph}), 134.7 (C_{Ph}), 134.6 (C_{Ph}), 129.3 (CH_{Ph}), 129.3 (CH_{Ph}), 129.1 (CH_{Ph}), 128.8 (CH_{Ph}), 128.4 (CH_{Ph}), 128.3 (CH_{Ph}), 128.1 (CH_{Ph}), 128.1 (CH_{Ph}), 127.9 (CH_{Ph}), 127.8 (CH_{Ph}), 126.5 (CH_{Ph}), 126.2 (CH_{Ph}), 126.1 (CH_{Ph}), 125.0 (CH_{Py}), 109.0 (CH_{Py}), 107.3 (CH_{Py}), 61.9 (CH_2), 54.8 (CH), 53.4 (CH), 53.4 (CH), 44.9 (CH_3), 38.2 (CH_2), 37.2 (CH_2), 37.1 (CH_2).

HRMS (ESI) m/z: Calcd for $C_{53}H_{50}N_7O_5^+$ 864.3868, Found 864.3877; Calcd for $C_{53}H_{49}N_7O_5Na_2^{2+}$ 454.6790, Found 454.6788; Calcd for $C_{53}H_{50}N_7O_5Na^{2+}$ 443.6880, Found 443.6879; Calcd for $C_{53}H_{51}N_7O_5^{2+}$ 432.6971, Found 432.6971.

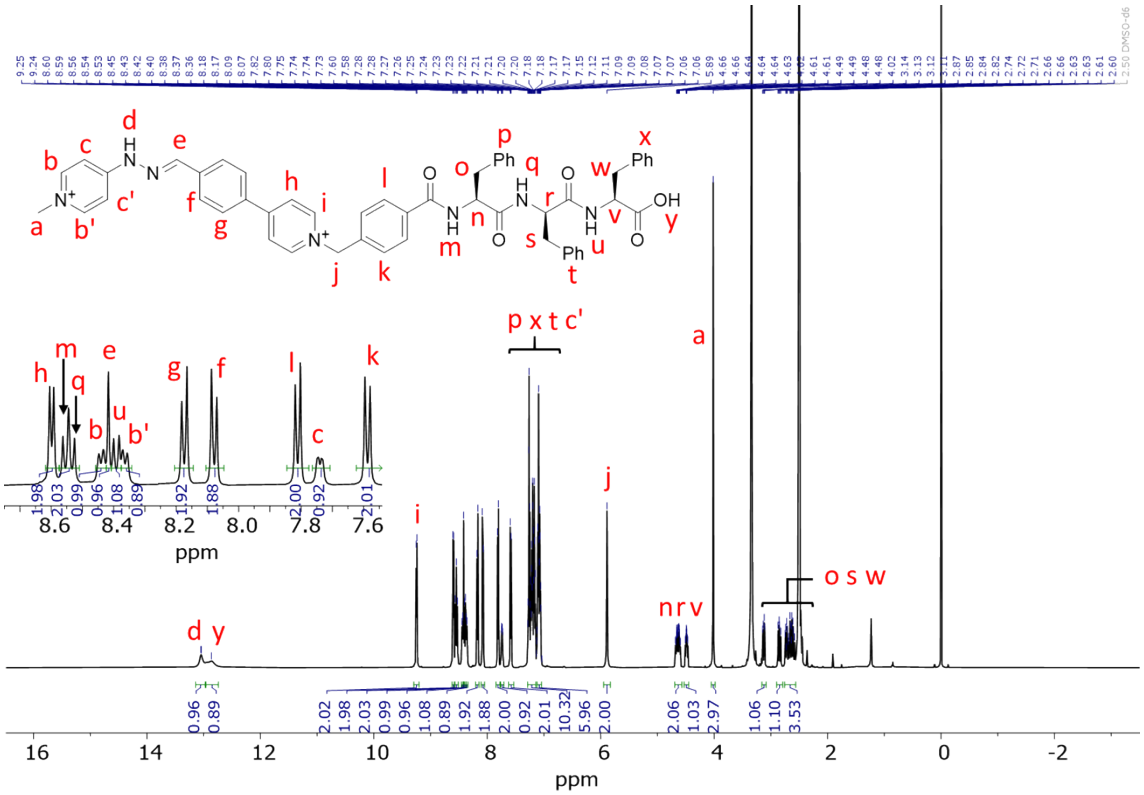

Fig. S16 ^{1}H NMR (500 MHz, DMSO-d6) spectrum of **2**. *Inset*: Scaling up of the 7.5-8.7 ppm range of the ^{1}H-NMR spectrum.

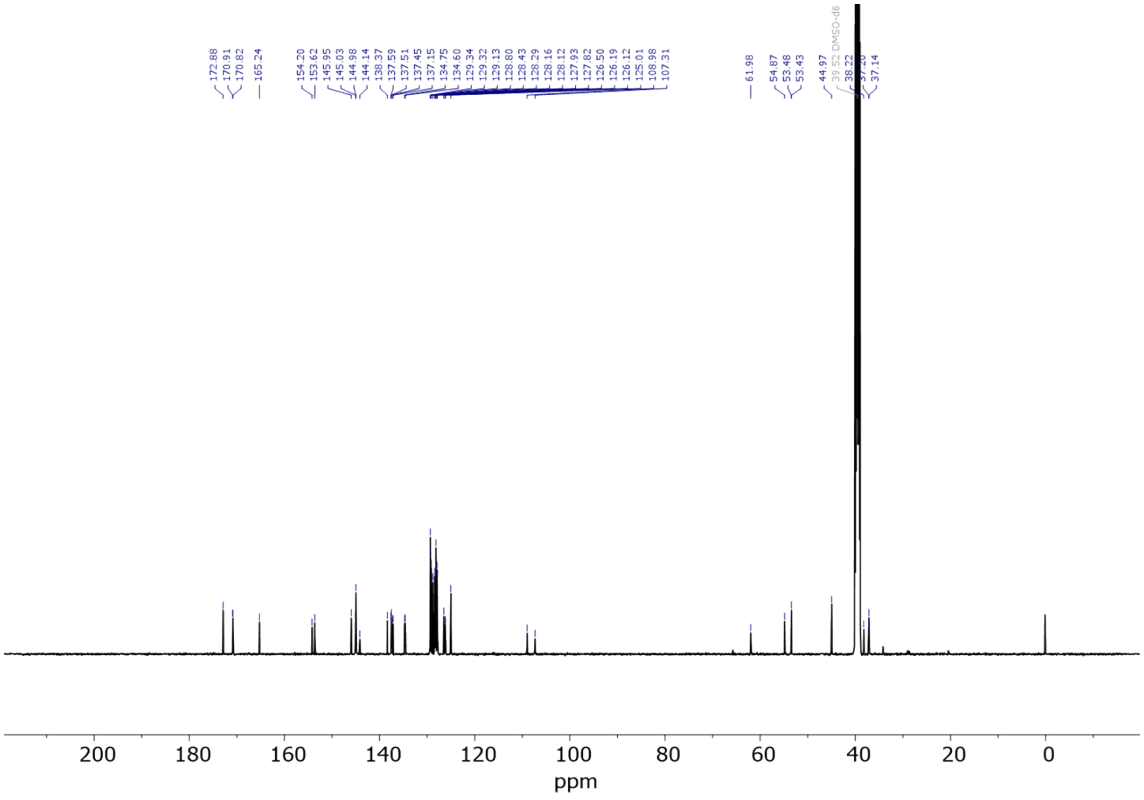

Fig. S17 ^{13}C{^{1}H} NMR (126 MHz, DMSO-d6) spectrum of **2**.

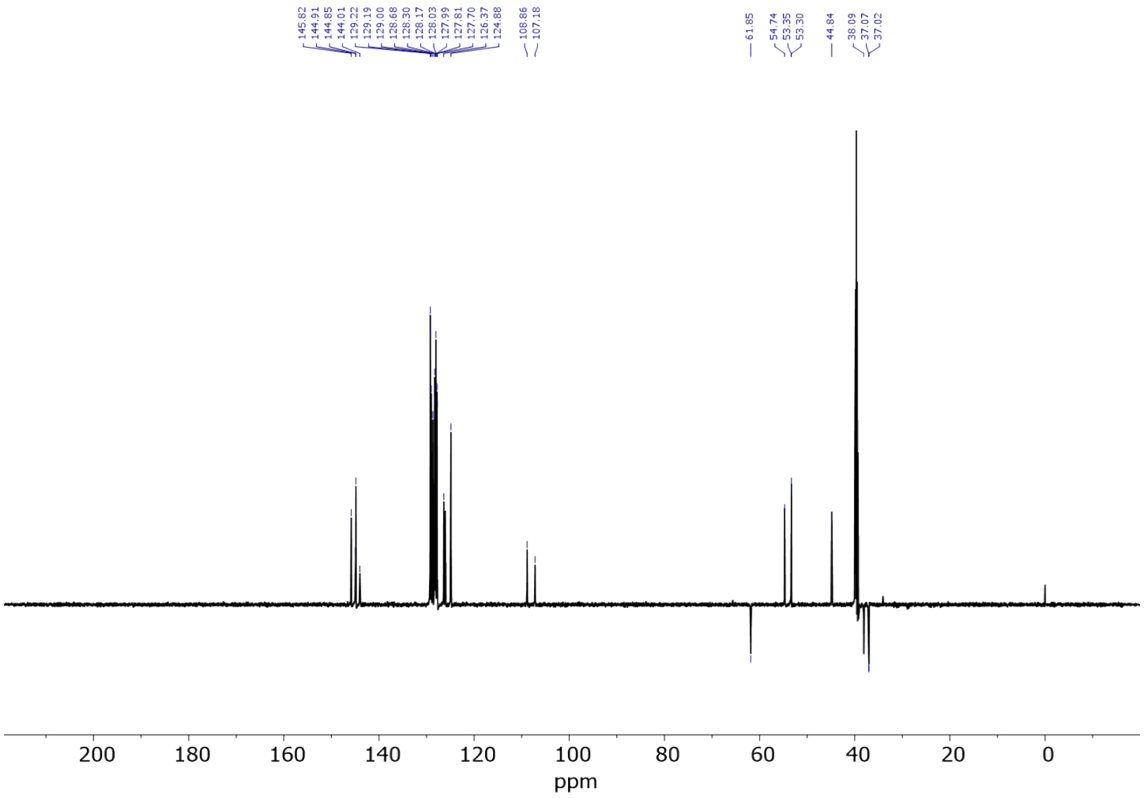

Fig. S18 DEPT-135 NMR (126 MHz, DMSO-d6) spectrum of **2**.

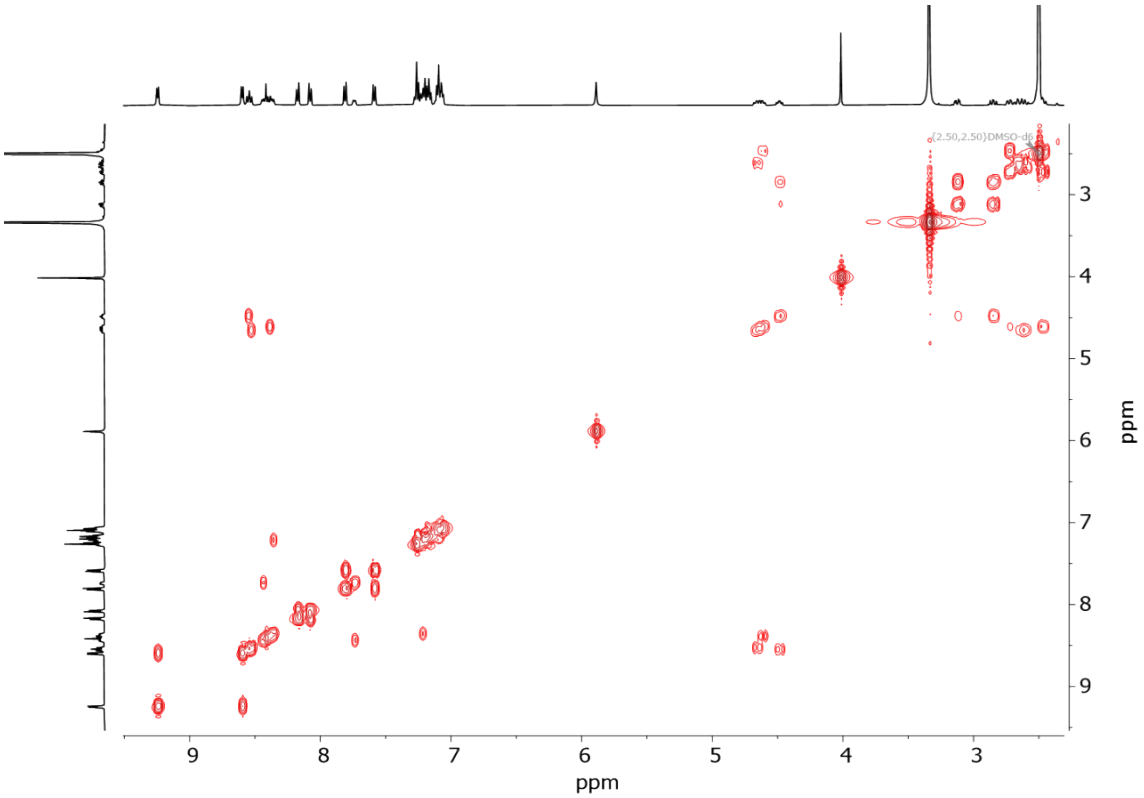

Fig. S19 ^{1}H-^{1}H COSY (500 MHz, DMSO-d6) spectrum of **2**.

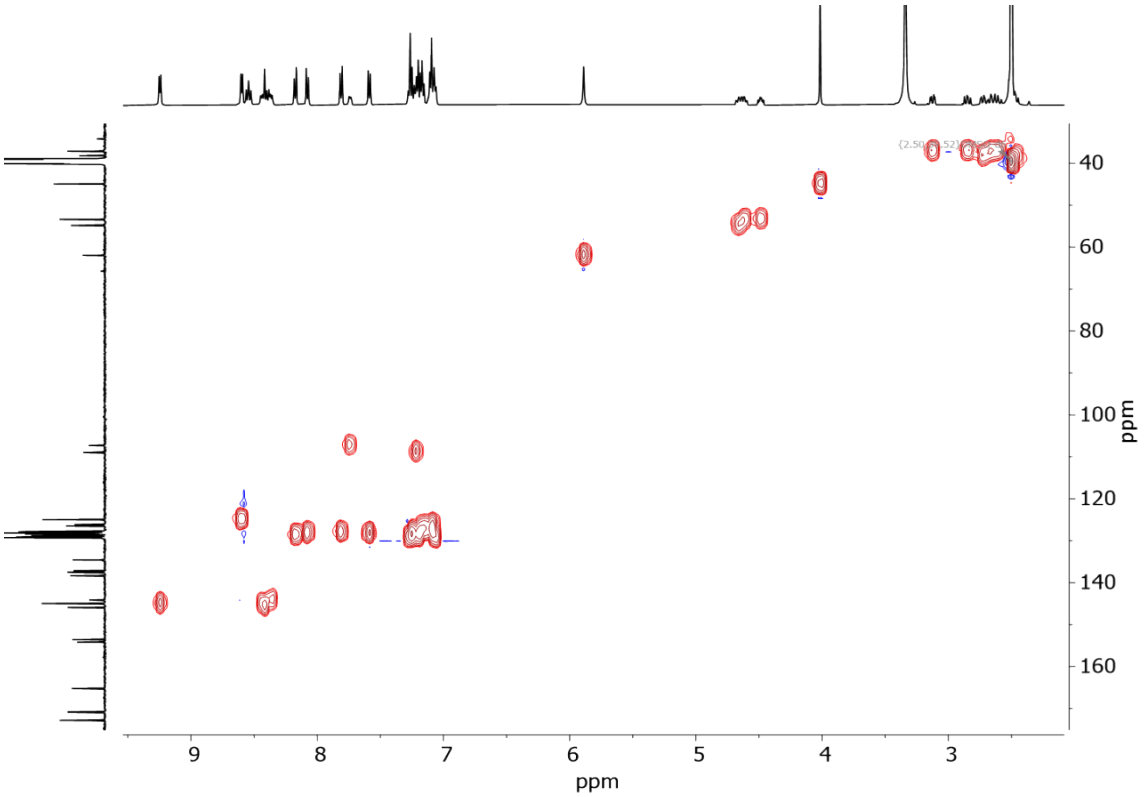

Fig. S20 ^{1}H-^{13}C HSQC (500 and 126 MHz, DMSO-d6) spectrum of **2**.

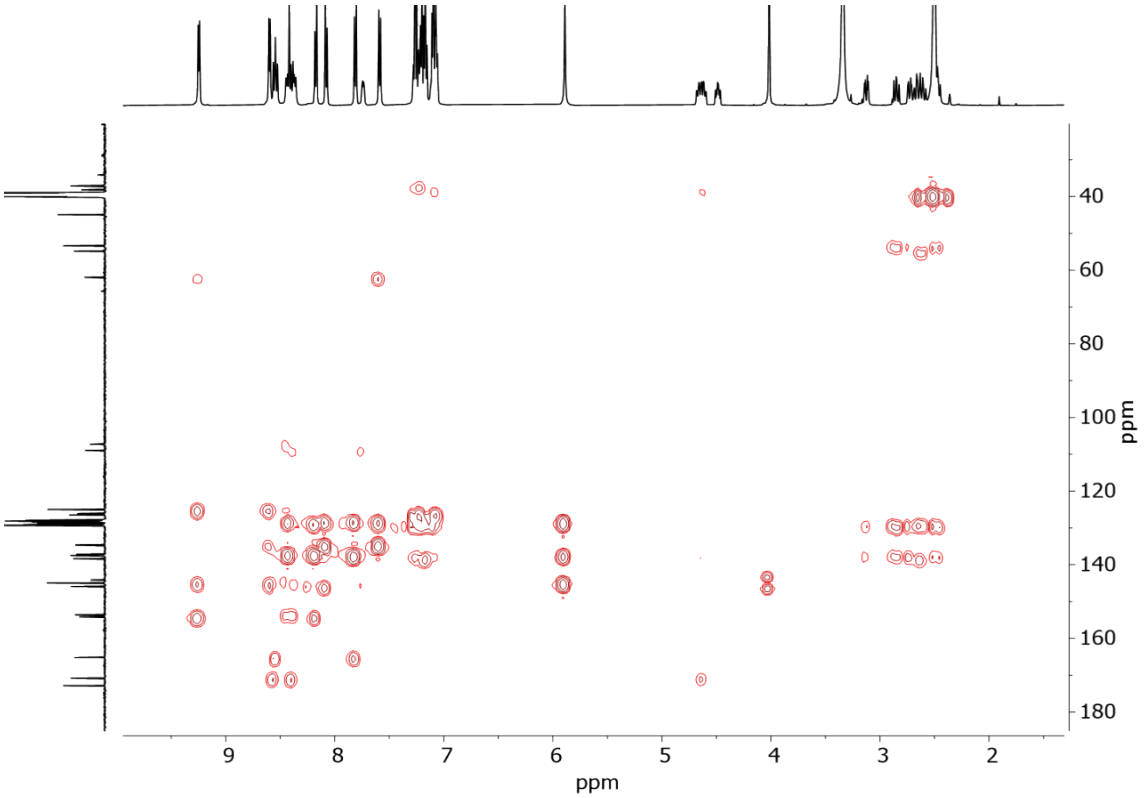

Fig. S21 ^{1}H-^{13}C HMBC (500 and 126 MHz, DMSO-d6) spectrum of **2**.

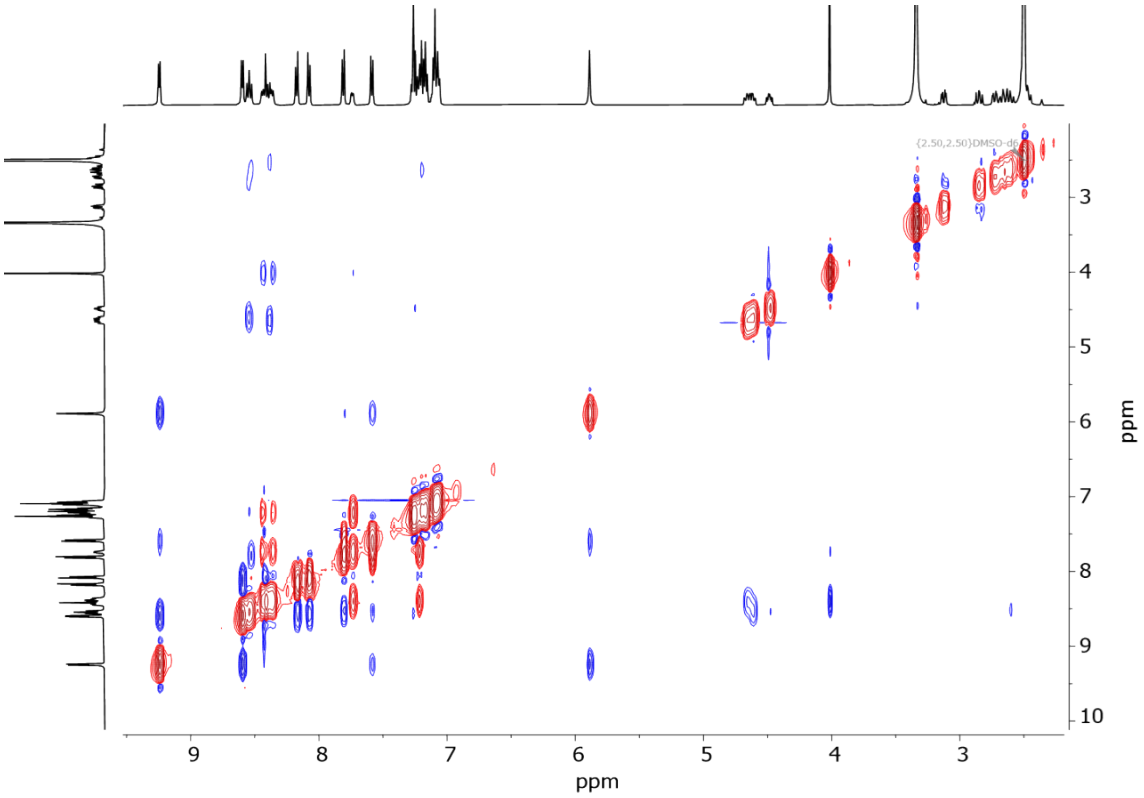

Fig. S22 ^{1}H-^{1}H NOESY (500 MHz, DMSO-d6) spectrum of **2**.

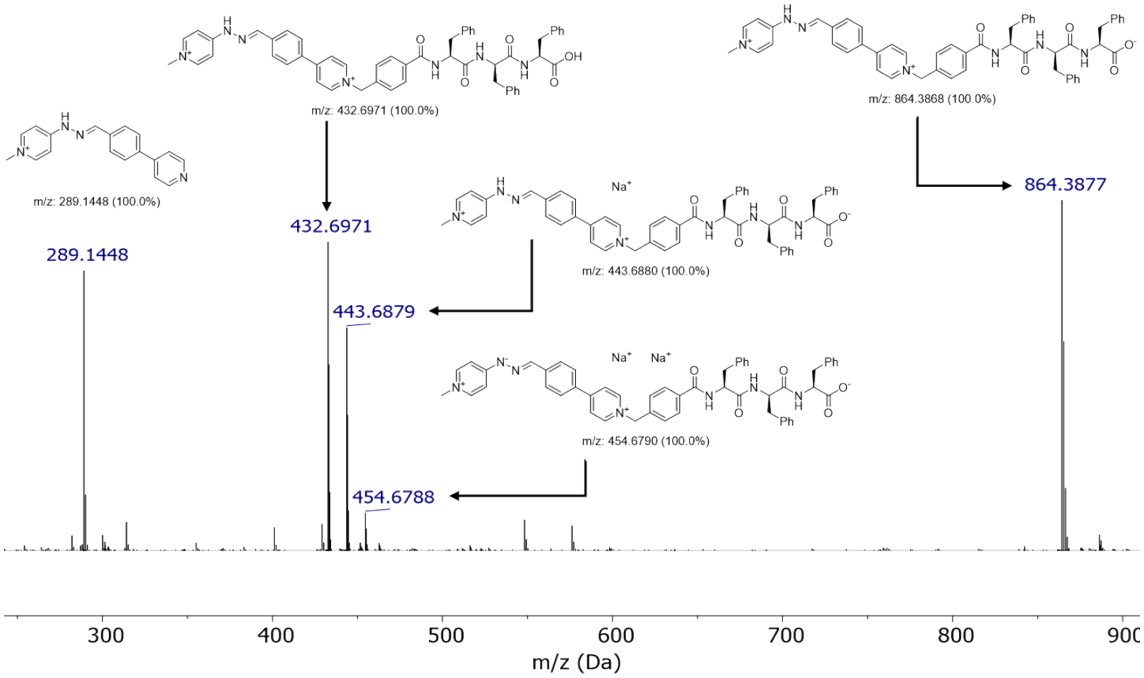

Fig. S23 HRMS-ESI spectrum of **2**.

S5. HPLC analysis.

1 and **2** were analyzed by HPLC (Thermo Scientific UltiMate 3000 connected to a photo-diode array detector) using a C-18 analytical column (Aeris, 3.6 µm, 100 Å, 150 x 2.1 mm^2, Phenomenex). Both compounds were dissolved in a mixture of 50/50 H_2O/MeCN with 0.04% TFA and analyzed using the same elution method (H_2O/MeCN con 0.04% TFA: *t* = 0–2 min, 5% MeCN; *t* = 23 min, 95% MeCN; *t* = 25–32 min, 95 % MeCN).

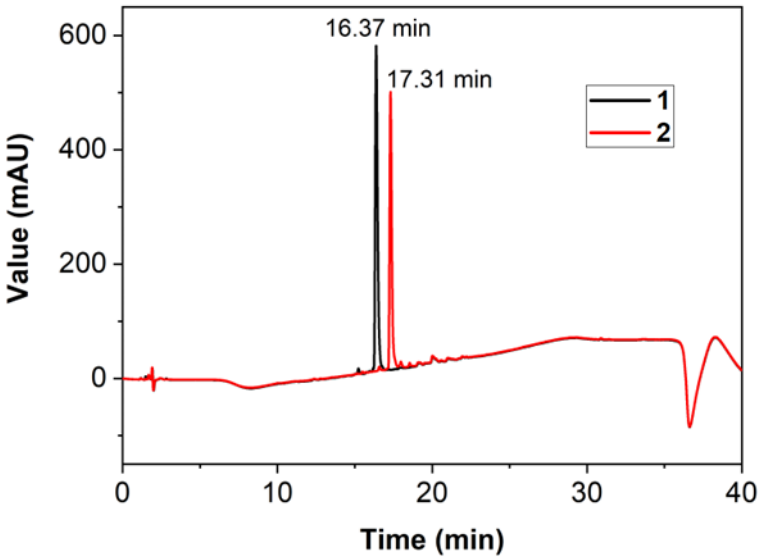

Fig. S24 Stacked HPLC chromatograms of **1** (black) and **2** (red).

S6. pK_a determination.

Potentiometric pH titration was carried out by dissolving **2** at a concentration of 10 mM in 0.4 mL of milli-Q water, followed by additions of NaOH (0.2 M), while monitoring the pH using a pH-meter microelectrode.

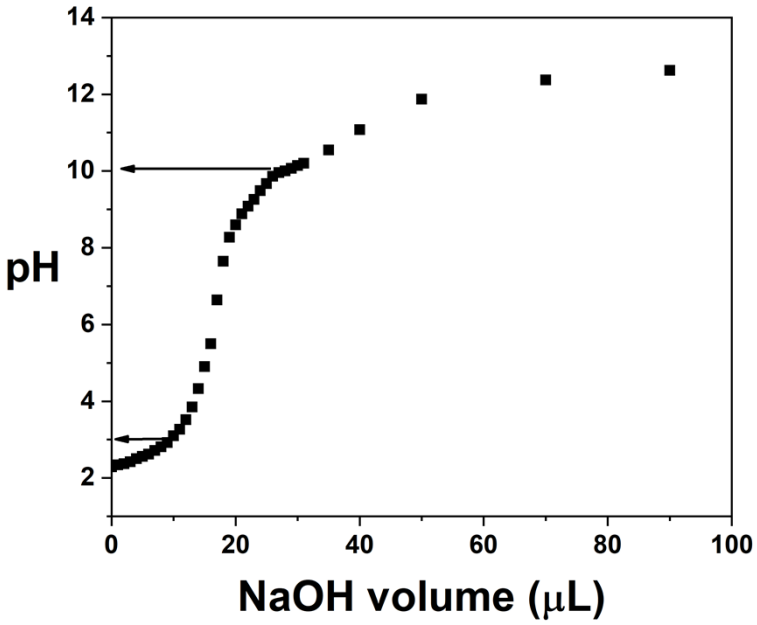

Fig. S25 Potentiometric pH titration for **2** at 10 mM.

S7. Hydrogels preparation.

2 is dissolved in aqueous phosphate buffer (0.1 M) at 10 mM in the range of pH 1-10. The resulting solution is left to gel at room temperature without the need of sonication or heating. The hydrogels prepared between pH 1 and 3 required at least 2 hours to gel, whereas those from pH 4 onwards only needed about 20–30 minutes, as verified by the vial inversion test.

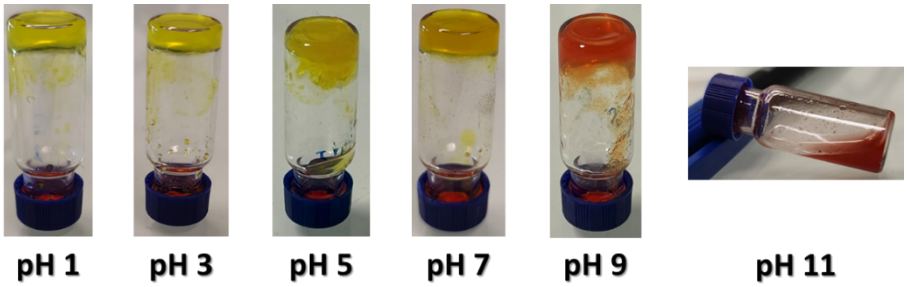

Fig. S26 Pictures of the hydrogels prepared in the pH range of 1-9 and de heterogeneous mixture at pH 11.

S8. UV-Vis characterization of 2.

Considering the calculated pK_a for compound **2**, UV–Vis absorption spectra were recorded for compound **2** at a concentration of 20 µM in 0.1 M phosphate buffer at pH 7 and pH 13. showing the characteristic shift of the $\pi \rightarrow \pi^*$ absorption band from 376 nm to 461 nm upon deprotonation.[2]

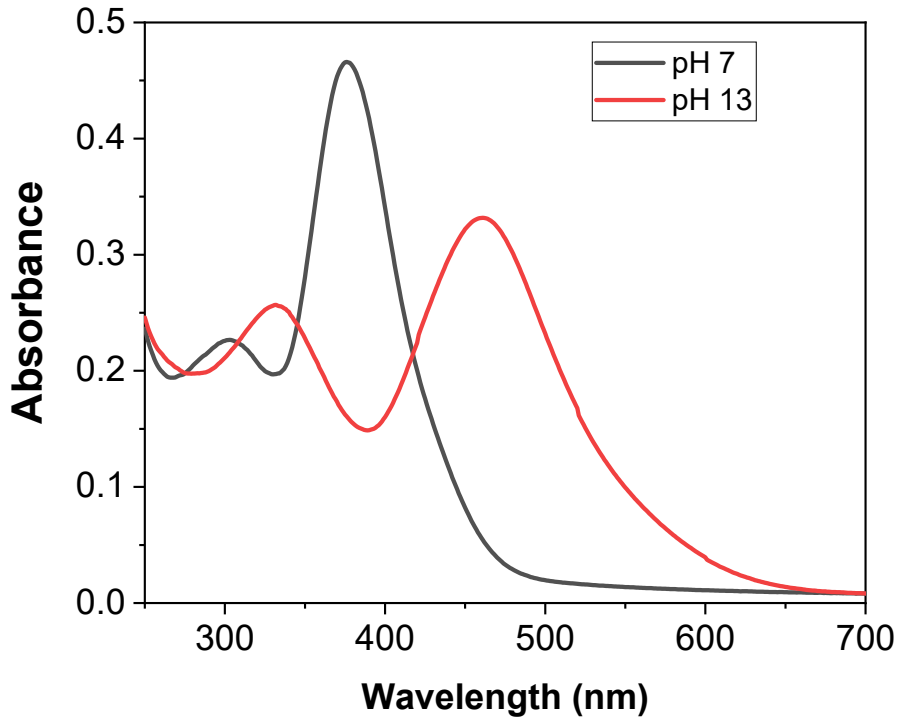

Fig. S27 UV–Vis absorption spectra of compound **2** recorded in 0.1 M phosphate buffer at pH 7 (black spectrum) and pH 13 (red spectrum).

S9. Rheology characterization of hydrogel at pH 7.

The hydrogel was prepared as described in Section S7 just before loading them into the rheometer. Measurement parameters for the time sweeps were set at 1 Hz and 1 Pa and for the frequency sweeps at 1 Pa. Time and frequency sweeps results are shown in Fig. 1C and 1D of the main text.

[2] L. Barravecchia, A. Blanco-Gómez, I. Neira, R. Skackauskaite, A. Vila, A. Rey-Rico, C. Peinador and M. D. García, *J. Am. Chem. Soc.*, 2022, **144**, 19127.

S10. TEM characterization.

The pseudopeptide was allowed to self-assemble for 1 hour at a concentration of 5 mM, and for 24 hours for samples prepared at concentrations ranging from 0.5 to 0.05 mM. Approximately 3 µL of the sample was carefully placed onto the carbon-coated film of a 300-mesh copper grid (Electron Microscopy Sciences, USA) and left to adsorb for 30 seconds. Excess liquid was removed by gently blotting one edge of the grid with absorbent paper. Immediately afterward, the grid was stained with 3 µL of 5% aqueous uranyl acetate for 30 seconds. Finally, the grid was rinsed with the appropriate phosphate buffer and dried under vacuum.

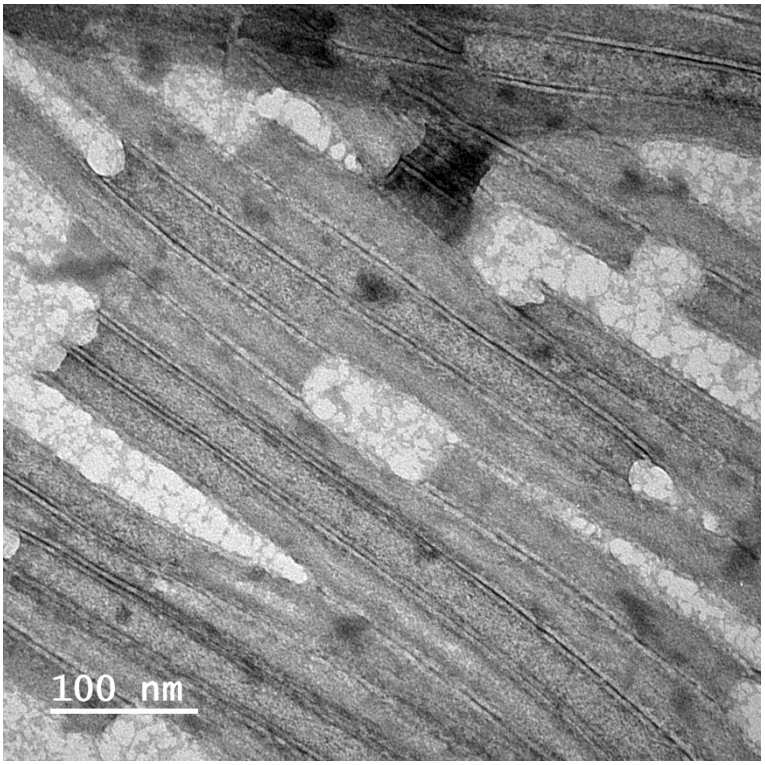

Fig. S28 TEM micrograph of **2** at 5 mM.

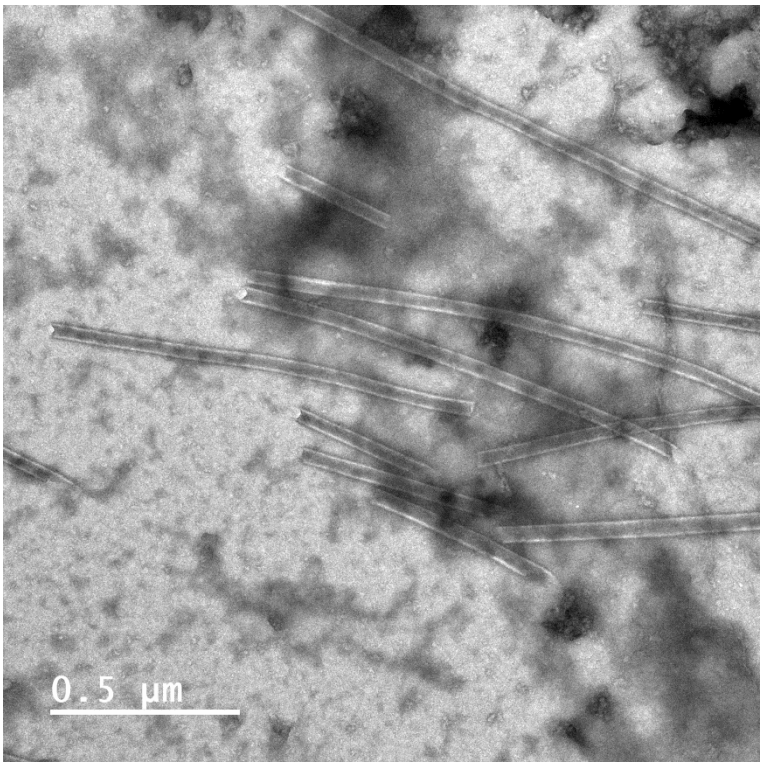

Fig. S29 TEM micrograph of **2** at 0.5 mM.

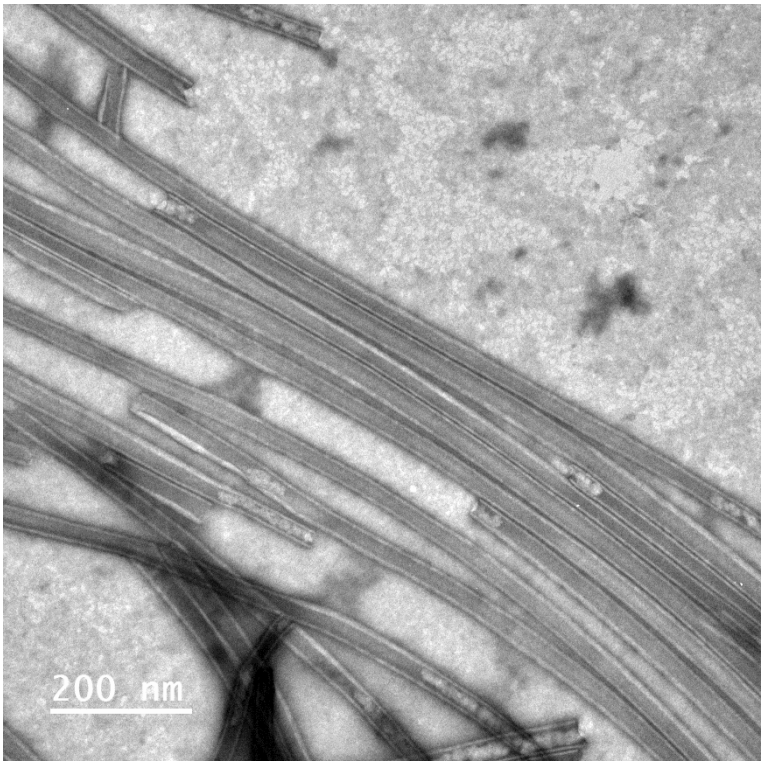

Fig. S30 TEM micrograph of **2** at 0.1 mM.

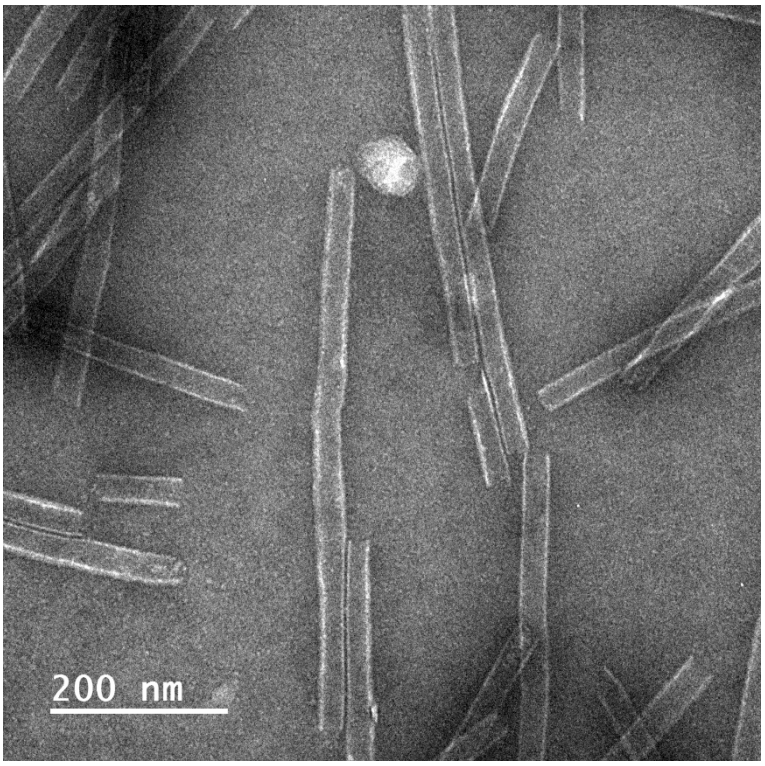

Fig. S31 TEM micrograph of **2** at 0.05 mM.

S11. SAXS data.

SAXS data for **2** was collected at concentrations ranging from 5 to 0.005 mM in phosphate buffer at pH 7 and 0.1 M. The sample was prepared in borosilicate glass capillaries (1.5 mm outer diameter, 0.01 mm wall thickness, WJM-Glas Müller GmbH). The experiment was conducted 36 hours after sample preparation at a temperature of 25 °C. Data acquisition took place at the NCD-SWEET beamline at ALBA Synchrotron (Spain). An X-ray energy of 12.5 keV was used, with the detector positioned 3.58 m from the sample, covering a scattering vector (q) range of 0.00486 to 0.417 $Å^{-1}$. Each measurement was set to 1 s exposure per frame, for a total of 30 frames. Due to evidence of radiation damage, only the first 15 frames were averaged for the final data file. Data reduction was performed using the PyFAI software.[3] Data averaging and background correction was done using the ATSAS software.[4] SAXS data and fittings are shown in Fig. 3A of the main text.

Table S1 Fitting models and optimal structural parameters for the SAXS data of **2** at different concentration, corresponding to Fig. 3A.

	2 5 mM	**2** 0.5 mM	**2** 0.01 mM
Model	Hollow cylinder	Hollow cylinder	Hollow cylinder
Scale	$1.4x10^{-6}±2.1x10^{-9}$	$1.4x10^{-7}±1.4x10^{-9}$	$3.0x10^{-8}±1.0x10^{-10}$
Background (cm^{-1})	$1.5x10^{-5}±4.9x10^{-8}$	$5.3x10^{-6}±3.4x10^{-8}$	$1.4x10^{-5}±4.0x10^{-8}$
Radius (Å)	125.9±0.1	132.2±0.2	125.7±0.3
Thickness (Å)	45.4±0.1	42.7±0.4	43[a]
Length (Å)	>1000	>1000	>1000
SLD ($x10^{-6}$ $Å^2$)[b]	13.4	13.4	13.4
SLD solvent ($x10^{-6}$ $Å^2$)[b]	9.4	9.4	9.4
χ^2	20	5	1

[a] Fixed parameter. [b] SLD and SLD solvent are the scattering length density of **2** and the solvent (H_2O + NaH_2PO_4 + Na_2HPO_4), respectively.

[3] J. Kieffer, J. Orlans, N. Coquelle, S. Debionne, S. Basu, Al. Homs, G. Santonia and D. De Sanctis, *J. Appl. Cryst.*, 2025, **58**, 138.

[4] K. Manalastas-Cantos, P. V. Konarev, N. R. Hajizadeh, A. G. Kikhney, M. V. Petoukhov, D. S. Molodenskiy, A. Panjkovich, H. D. T. Mertens, A. Gruzinov, C. Borges, C. M. Jeffries, D. I. Svergun and D. Franke, *J. Appl. Cryst.*, 2021, **54**, 343.

S12. FTIR characterization.

Pseudopeptides **1** and **2** are separately dissolved at a concentration of 5 mM in phosphate buffer solutions at pD 6 and pD 7, respectively. Both solutions are allowed to gel for 1 hour. Then, 100 µL of the resulting hydrogel is placed between two CaF_2 windows using a 50 µm spacer (Omni Cell demountable liquid cell). The background, buffer solutions at pD 6 and 7, and the samples are recorded with 25 scans and a resolution of 1 cm^{-1}.

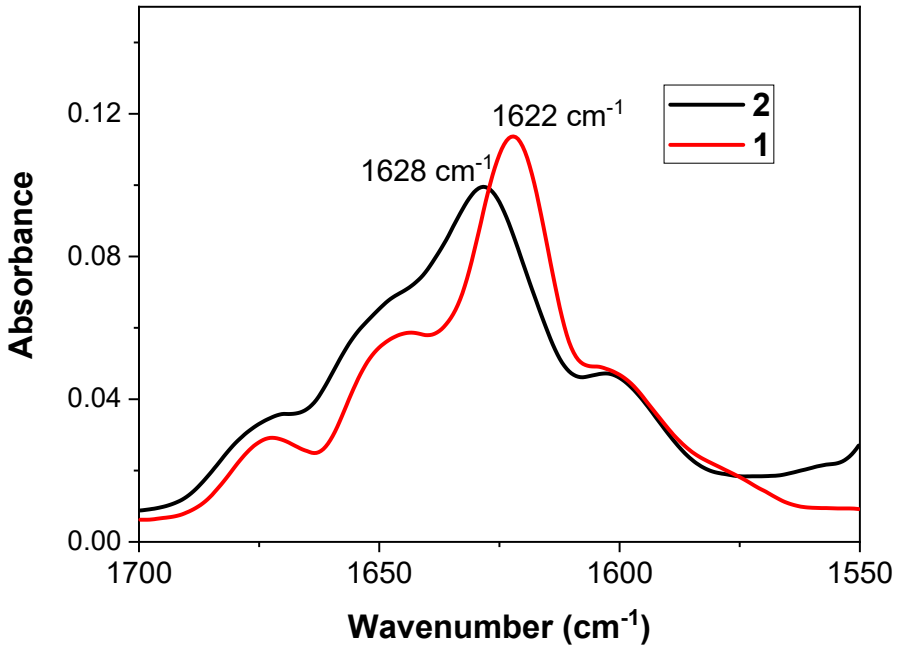

Fig. S32 IR spectra of the amide-I region for hydrogels prepared at 5 mM and pD 6 and 7 of **1** (red spectrum) and **2** (black spectrum), respectively.

S13. Circular dichroism studies.

Samples were measured in quartz cuvettes with different path lengths depending on the concentration:

- For concentrations between 5 and 0.5 mM, a 0.01 cm cuvette was used.
- For concentrations between 0.5 and 0.1 mM, a 0.1 cm cuvette was used.
- For concentrations between 0.025 and 0.005 mM, a 0.2 cm cuvette was used.

The spectrum of **2** at 5 mM was recorded immediately after dissolving the compound in the buffer at pH 7. Samples with concentrations between 0.5 and 0.005 mM were measured after 24 hours (spectra are shown in the main text).

CD data is reported in molar ellipticity [Θ] in deg cm^2 $dmol^{-1}$.

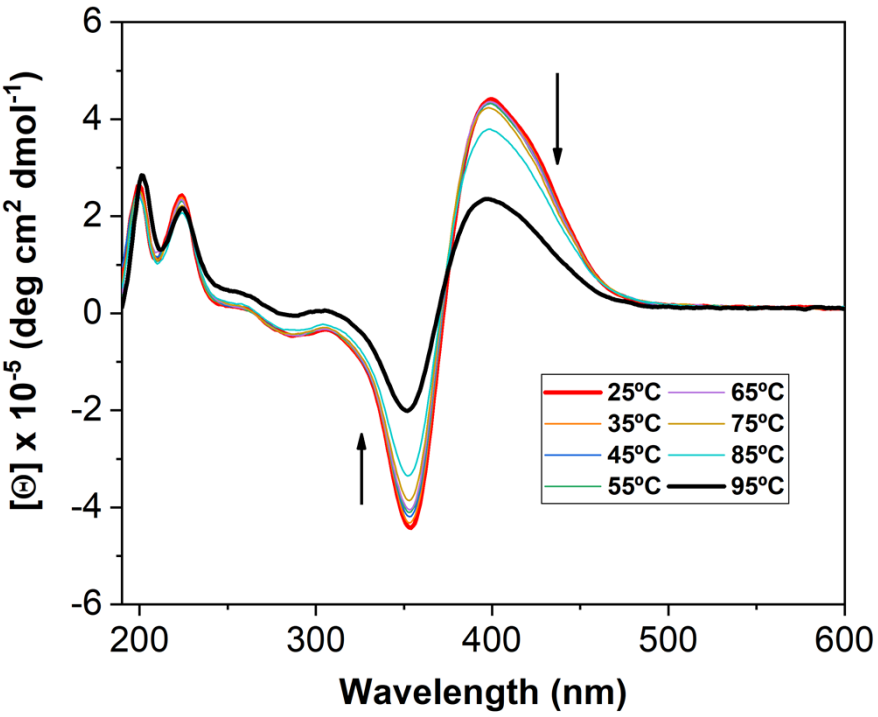

Fig. S33 CD spectra of **2** hydrogel at 5 mM and pH 7 recorder at different temperatures.

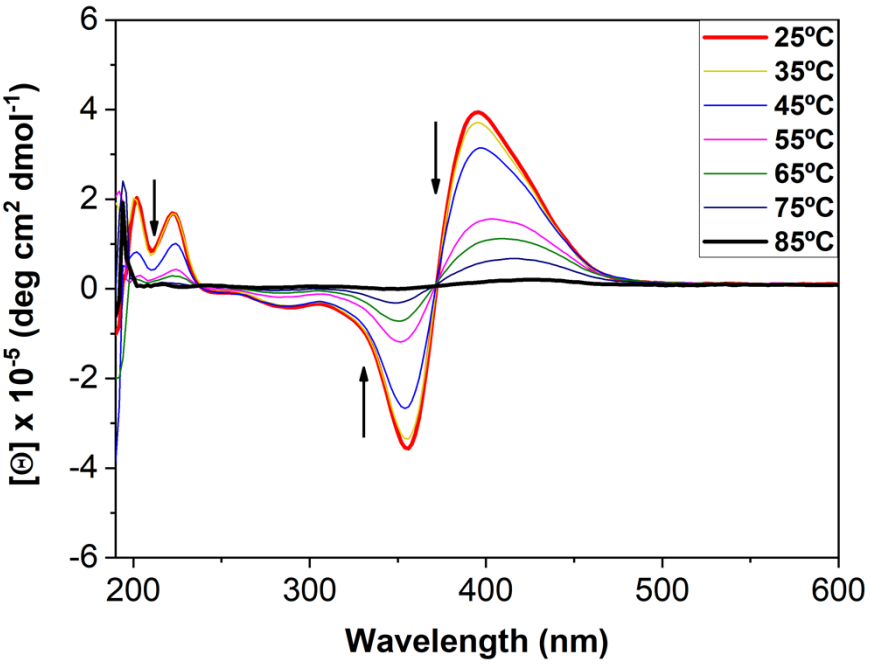

Fig. S34 CD spectra of **2** at 0.1 mM and pH 7 recorder at different temperatures.

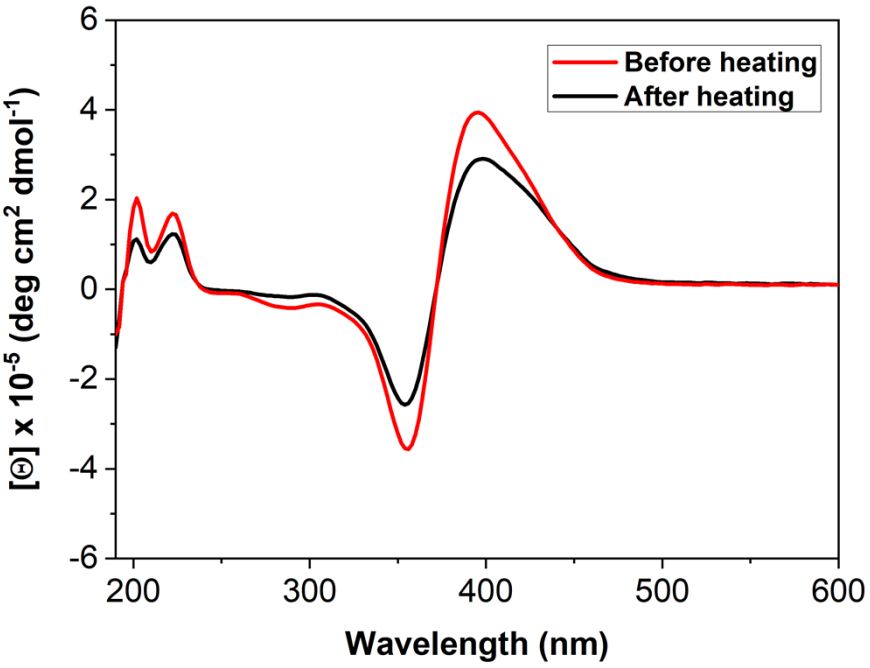

Fig. S35 CD spectra of **2** at 0.1 mM and pH 7 recorder before heating until 85 °C (red spectrum) and after heating until 85 °C and cooling at room temperature during 30 min (black spectrum).

S14. TEM characterization after thermal treatment.

TEM analysis was carried out on the sample after completion of the CD thermal experiments up to 85 °C (Fig. S35). The TEM micrograph (Fig. S36) reveals that the nanostructured morphology is preserved even after exposure to high temperatures, indicating the thermal robustness of the assembled structure.

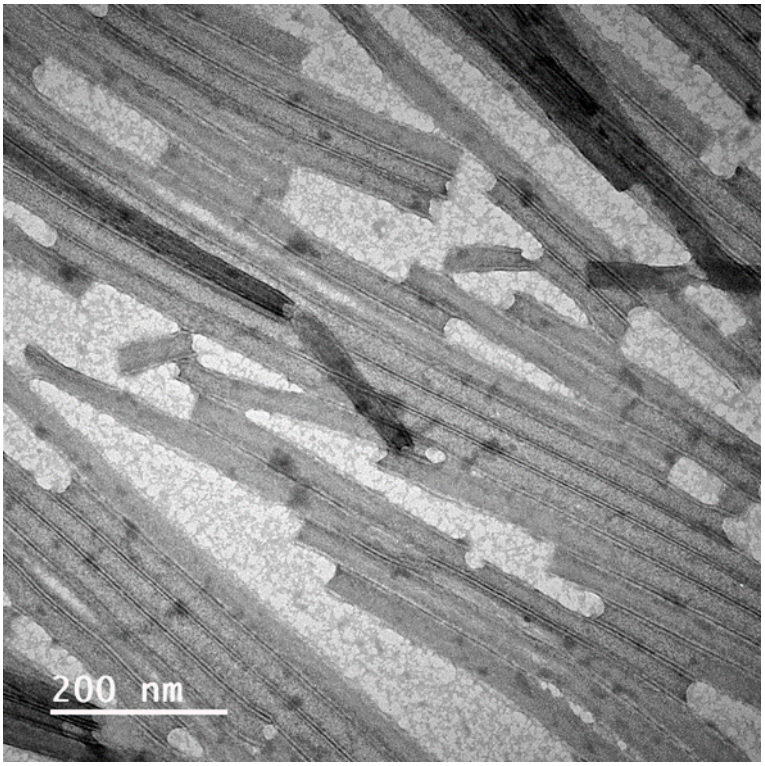

Fig. S36. TEM micrograph of **2** at 0.1 mM after heating until 85 °C and cooling at room temperature.

S15. Time-dependent stability studies.

Time-dependent stability studies were conducted by comparing circular dichroism and TEM data acquired at two different time points: immediately after sample preparation and after incubation for three weeks at 37 °C. Both the gel sample (5 mM) and the nanotube suspension (0.1 mM), prepared in 0.1 M phosphate buffer at pH 7, were subjected to this stability assessment.

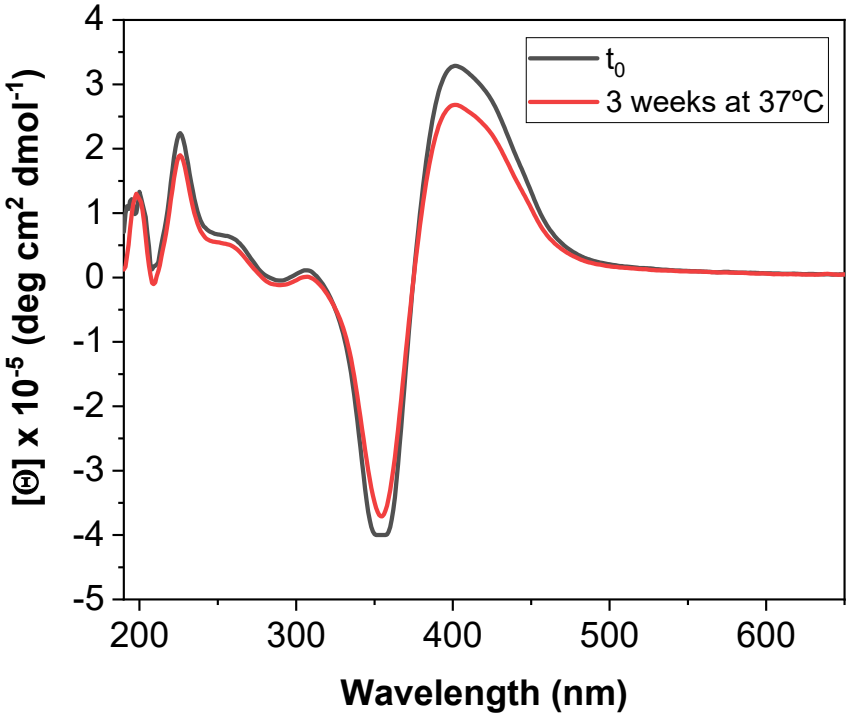

Fig. S37 CD spectra comparison of **2** at 5 mM recorded immediately after sample preparation (black spectrum) and after incubation at 37 °C for three weeks (red spectrum).

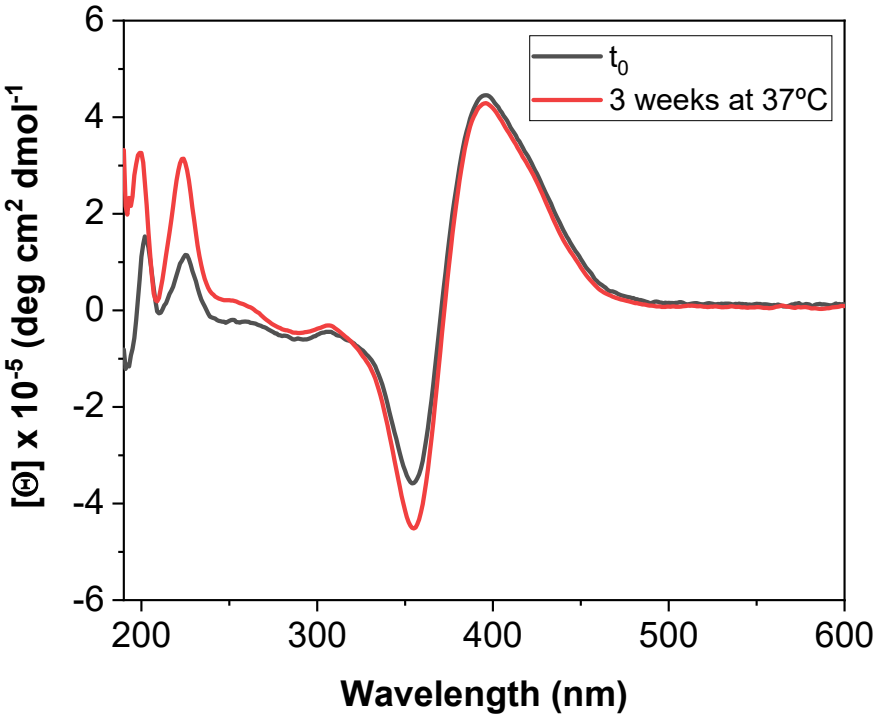

Fig. S38 CD spectra comparison of **2** at 0.1 mM recorded immediately after sample preparation (black spectrum) and after incubation at 37 °C for three weeks (red spectrum).

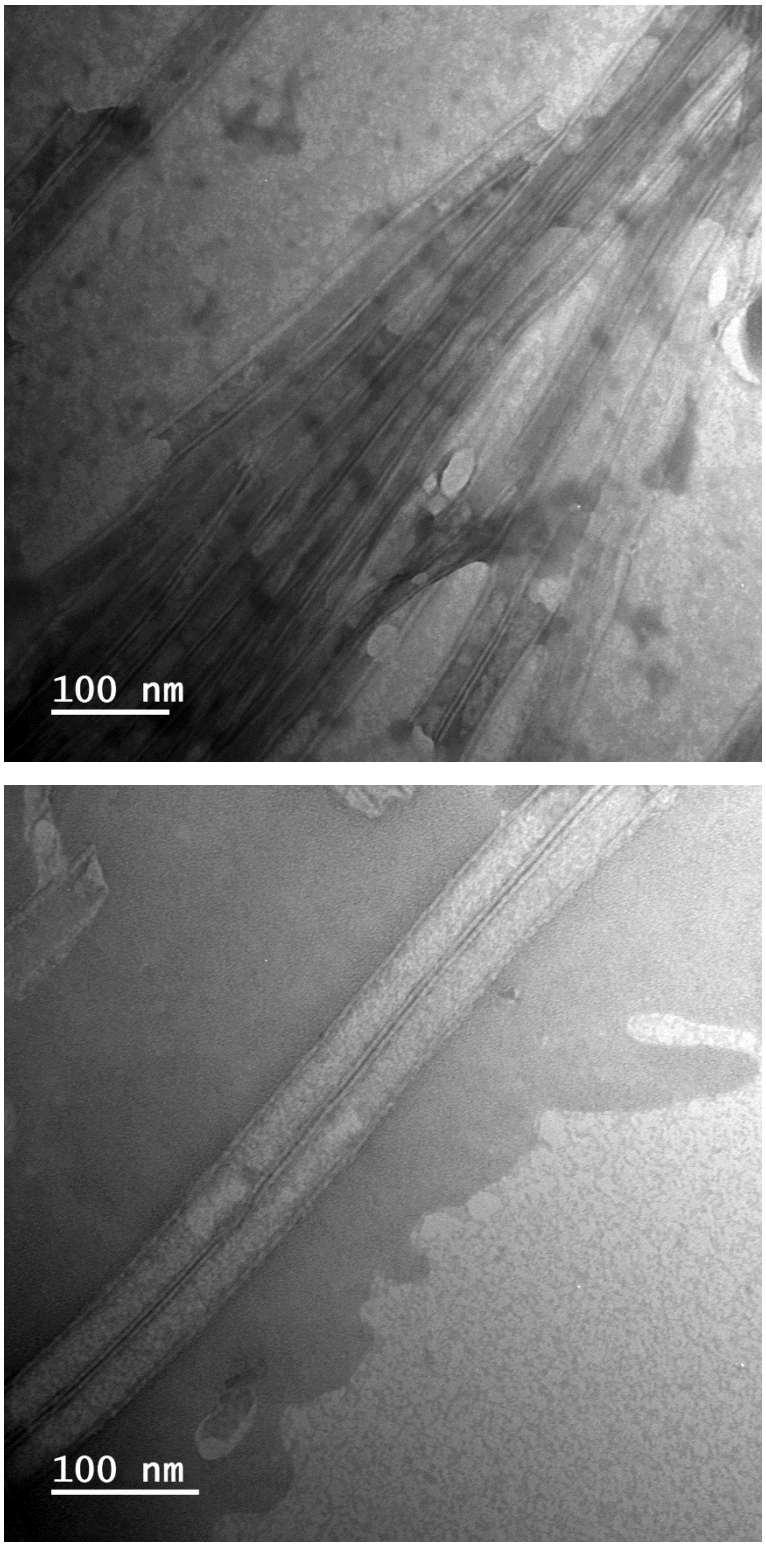

Fig. S39 TEM micrograph of **2** at 0.1 mM after incubation at 37 °C for three weeks.

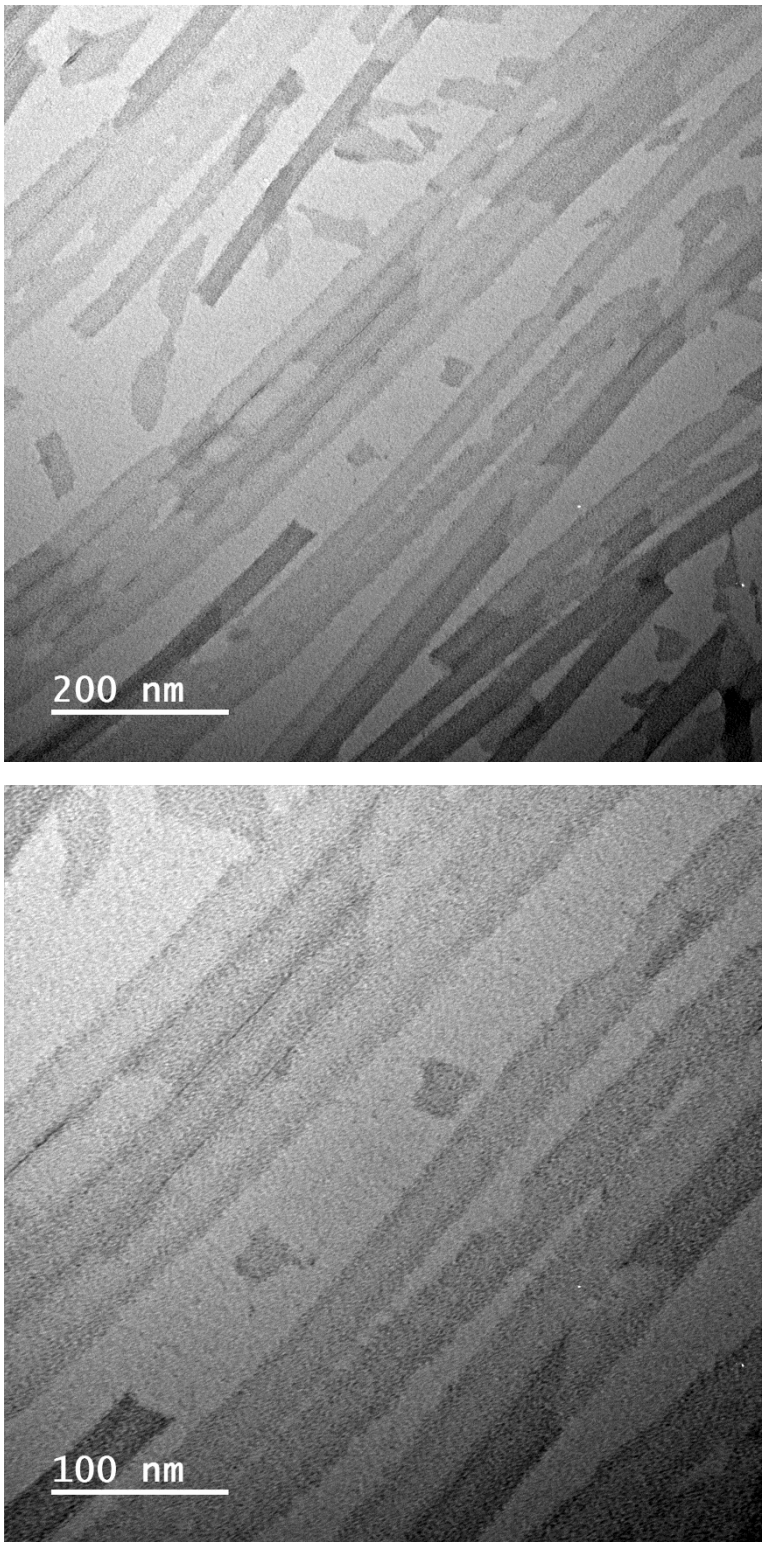

Fig. S40 TEM micrograph of **2** at 5 mM after incubation at 37 °C for three weeks.

S16. Interaction studies of nanotubes with fluorophores.

Studies with pyranine.

First, a 0.2 mM solution of **2** was prepared in 0.1 M phosphate buffer at pH 7 and allowed to self-assemble into nanotubes over a period of 24 hours. From this stock solution, a series of **2** solutions at 0.1 mM were prepared in the same pH 7 phosphate buffer, containing increasing concentrations of pyranine ranging from 0.01 to 0.1 mM. In parallel, identical pyranine solutions were prepared in the absence of **2** to serve as controls. All resulting solutions were gently stirred at room temperature for approximately 1 hour before measurements.

For the CD experiments, the samples were measured in a quartz cuvette with a 0.1 cm path length. For the fluorescence experiments, a quartz cuvette with a 1 cm path length was used, with an λ_{EX} of 450 nm, and both excitation and emission slits set to 2.5 nm.

As shown in Fig. S35, the emission of pyranine in the presence of the self-assembled **2** nanotubes undergo strong quenching, with over 80% fluorescence reduction up to a molar ratio of 0.3:1 (pyranine/**2**) and reaching saturation at about 50% at a 1:1 ratio. These findings suggest a strong interaction between the anionic fluorophore and the cationic surface of the nanotubes via electrostatic or/and π–π interactions. Meanwhile, the circular dichroism spectra (Fig. S36) reveals that the overall chiral structure of the assembly is preserved, although with a gradual decrease in band intensity as the pyranine concentration increases. This variation might indicate that fluorophore binding alters the supramolecular stacking and chirality, likely through intercalation or superficial insertion of its aromatic ring between the bispyridinium units.

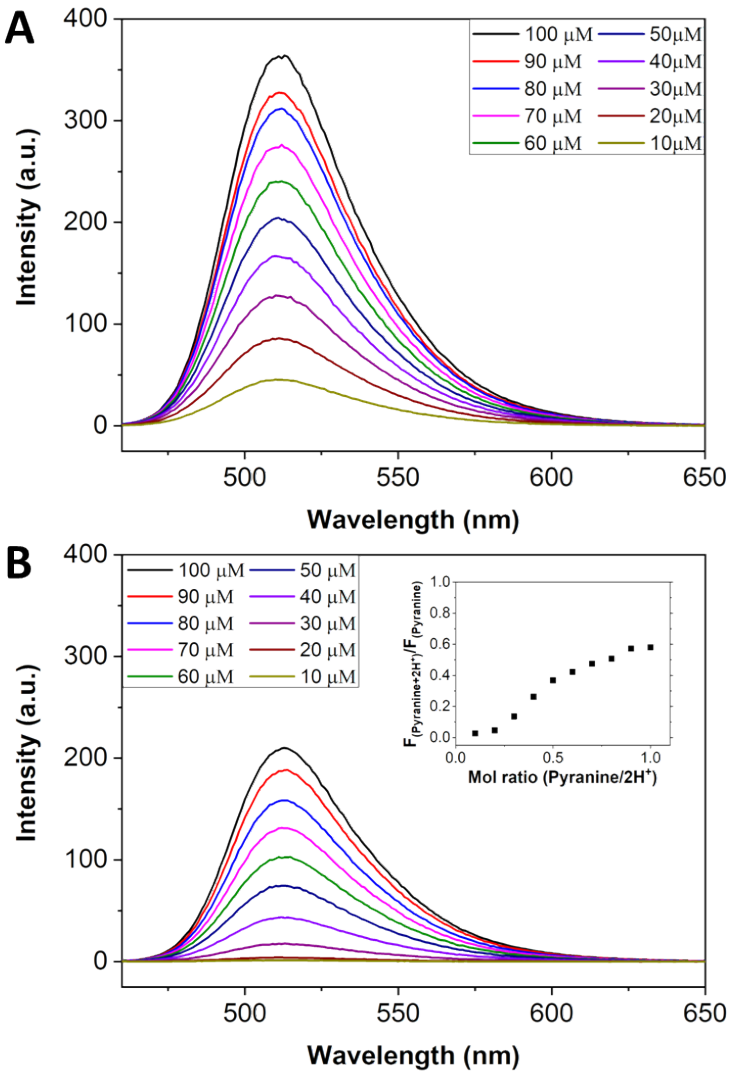

Fig. S41 Fluorescence spectra of pyranine at concentrations ranging from 10 to 100 μM, in the absence of **2** (A) and in the presence of 100 μM **2** (B). *Inset* in Fig. S41B shows the variation in pyranine fluorescence intensity (515 nm) as a function of the pyranine/**2** molar ratio.

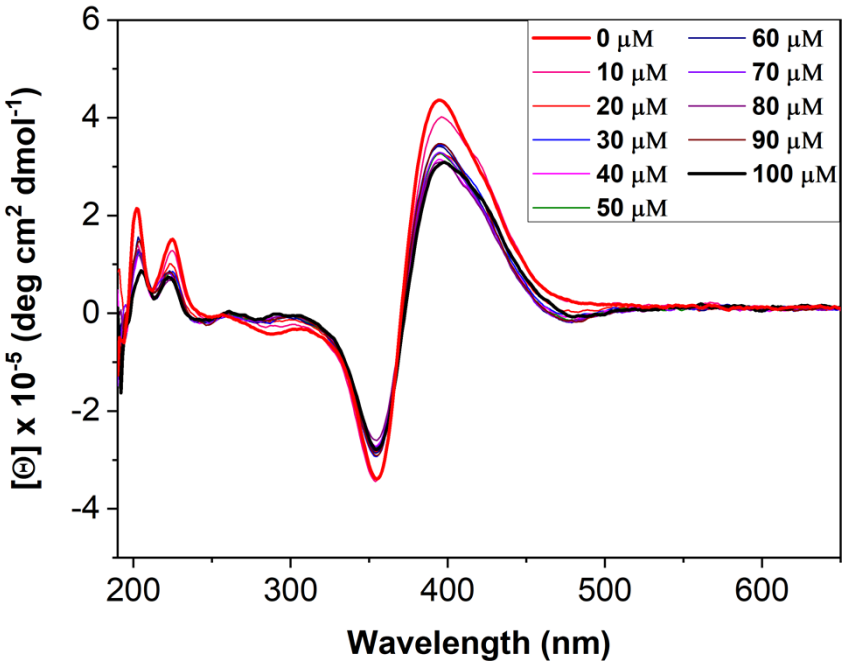

Fig. S42 CD spectra of **2** at 0.1 mM in the presence of different concentrations of pyranine.

Studies with Nile Red (NR).

A 0.1 mM solution of **2** is prepared and allowed to self-assemble for 24 hours. In parallel, a 1.2 mM solution of **NR** in CH_2Cl_2 is prepared. From this solution, different volumes are transferred into several vials, and the solvent is allowed to evaporate. Subsequently, 2.5 mL of the 0.1 mM **2** solution is added to the **NR** residue in each vial, and all mixtures are stirred at room temperature for 24 hours.

For the CD experiments, the samples were measured in a quartz cuvette with a 0.1 cm path length. For the fluorescence experiments, a quartz cuvette with a 1 cm path length was used, with an λ_{EX} of 588 nm, and both excitation and emission slits set to 5 nm.

As shown in Fig. S37, neither an increase nor a significant change in the fluorescence of the neutral fluorophore **NR** is observed upon interaction with the self-assembled nanotubes of **2**. This result contrasts with that observed for other nanotubes that possess hydrophobic cavities capable of encapsulating **NR**, which commonly induces an increase in emission.[5] Additionally, the CD spectrum in Fig. S38 confirms that the secondary structure of **2** remains unaltered in the presence of **NR**, indicating a lack of significant interaction between the fluorophore and the supramolecular structure.

[5] F. Aparicio, P. B. Chamorro, R. Chamorro, S. Casado, and D. González-Rodríguez, *Angew. Chem. Int. Ed.*, 2020, **59**, 17091.

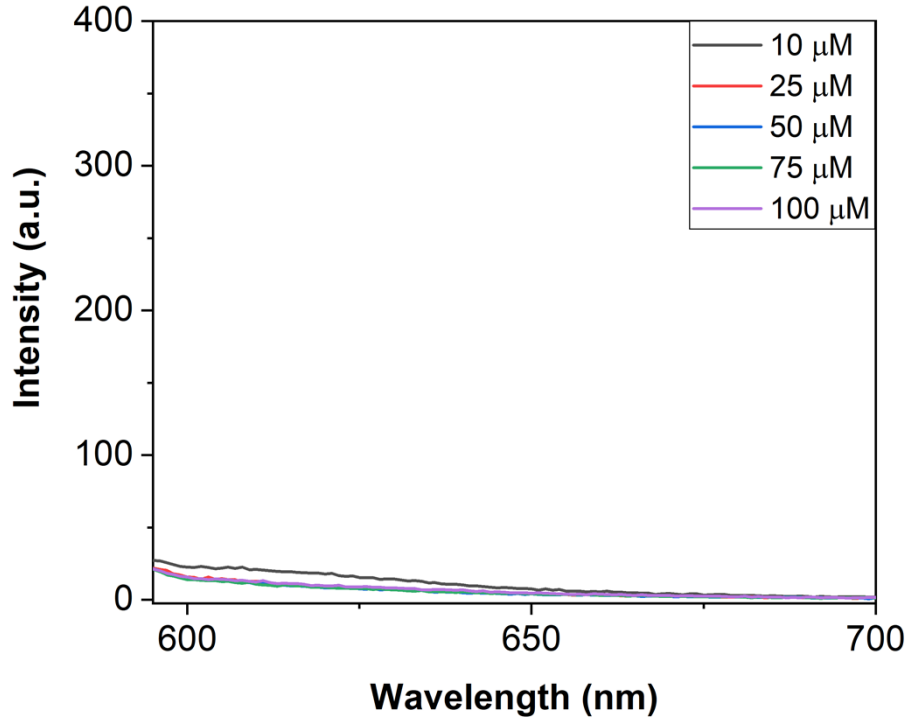

Fig. S43 Fluorescence spectra of **NR** at concentrations ranging from 10 to 100 μM in the presence of 100 μM **2**.

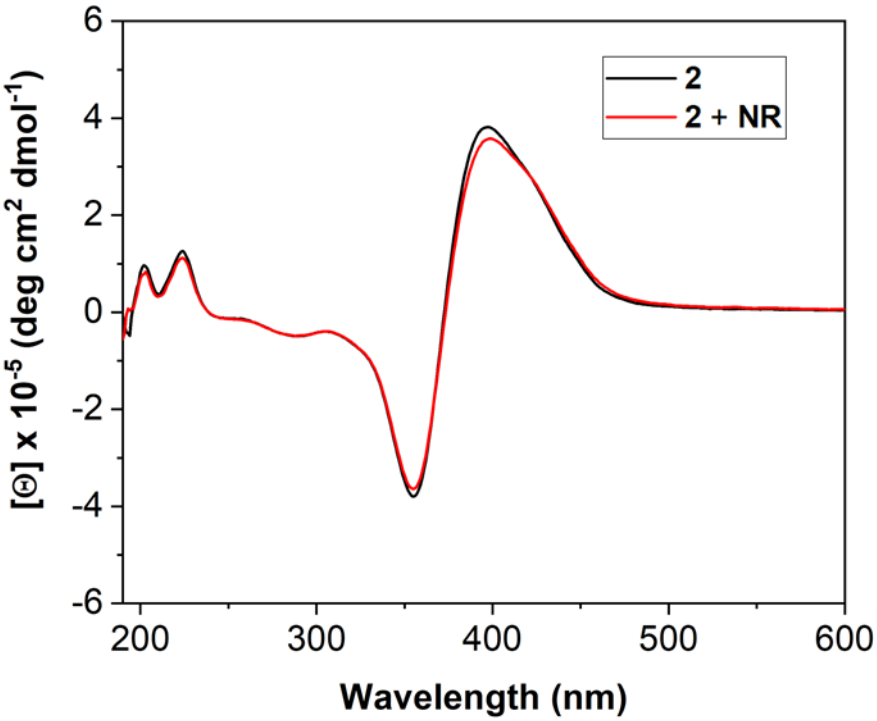

Fig. S44 CD spectra of **2** at 0.1 mM in absence (black spectrum) and presence of Nile Red at 0.1 mM (red spectrum).

Studies with berberine (BB).

First, a 0.2 mM solution of **2** was prepared in 0.1 M phosphate buffer at pH 7 and allowed to self-assemble into nanotubes over a period of 24 hours. From this stock solution, a series of **2** solutions at 0.1 mM were prepared in the same pH 7 phosphate buffer, containing increasing concentrations of berberine ranging from 0.01 to 0.1 mM. All resulting solutions were gently stirred at room temperature for approximately 1 hour before measurements.

For the CD experiments, the samples were measured in a quartz cuvette with a 1 mm path length. For the fluorescence experiments, a quartz cuvette with a 10 mm path length was used, with an λ_{EX} of 450 nm, and both excitation and emission slits set to 5 nm.

Similar to **NR**, **BB** showed no significant interaction with the self-assembled **2** nanotubes. The fluorescence studies show no increase in **BB** emission (Fig. S39), suggesting that the cationic surface of the nanotube prevents the interaction. This is contrary to the fluorescence enhancement **BB** typically undergoes when binding to anionic structures (such as G4-DNA).[6] The lack of interaction is further confirmed by CD (Fig. S40), where the spectra of **2** with and without **BB** completely overlap.

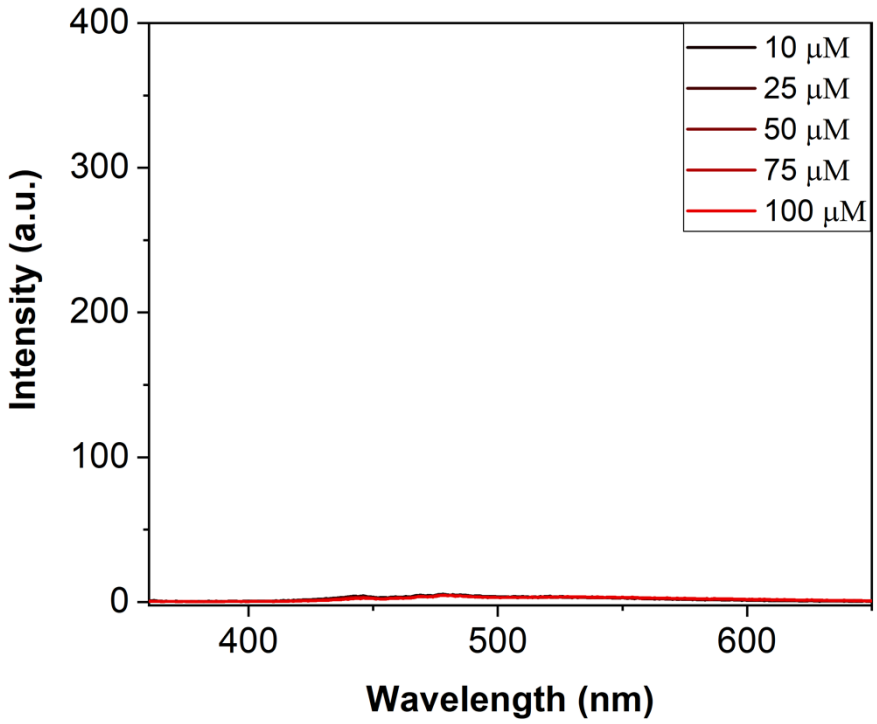

Fig. S45 Fluorescence spectra of **BB** at concentrations ranging from 10 to 100 μM in the presence of 100 μM **2**.

[6] J. Dickerhoff, N. Brundridge, S. A. McLuckey, and D. Yang, *J. Med. Chem.*, 2021, **64**, 16205.

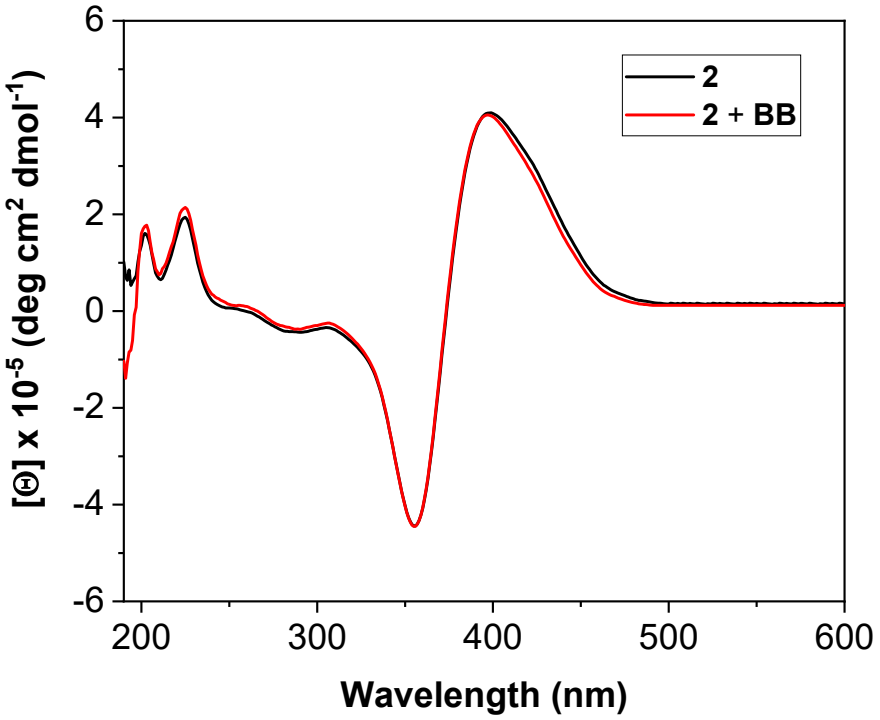

Fig. S46 CD spectra of **2** at 0.1 mM in absence (black spectrum) and presence of **BB** at 0.1 mM (red spectrum).

S17. Computational details.

All calculations reported herein were performed using the software ORCA 6.1.0.[7]

To hypothetically estimate the thickness of the β-sheet bilayer that constitutes the nanotube wall, a dimer of **2** was modeled with a specific orientation, based on the following considerations and approximations:

1) The initial structural model was taken from the conformation observed in single-crystal XRD data of the analogous compound **1**.[8] This structure displays a torsion in the peptide backbone that facilitates interaction in a parallel β-sheet motif, which has also been characterized in **2** by FTIR spectroscopy (Fig. S31).
2) The bipyridinium unit of the starting model (**1**) was replaced by the bipyridinium unit corresponding to the **2** pseudopeptide with the software chimeraX.
3) The two **2** units were oriented so that the Phe groups pointed inward, emulating the hydrophobic core of the bilayer, while the bipyridinium units remained exposed, representing the bilayer surface.

The initial geometry, generated as described above, was optimized at the r²SCAN-3c[9](CPCM[10] (water)) level of theory, with the geometry (Figure S41) corroborated as a minimum on the corresponding potential energy surface by frequency analysis. Cartesian coordinates for the optimized structure can be found in xyz format within the supplementary file structure.zip.

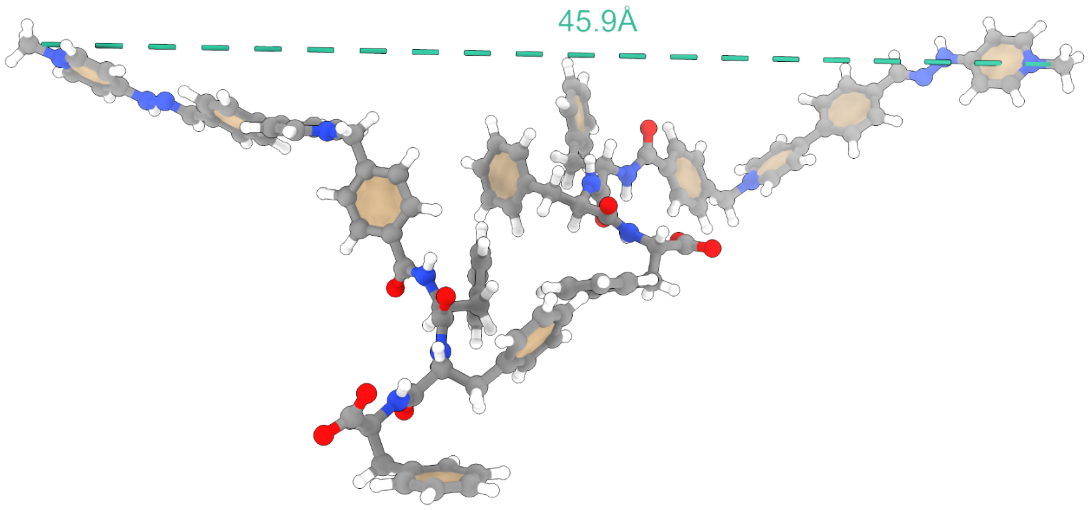

Fig. S47 Ball and stick representation of the geometry of dimer $(\mathbf{2})_2$, optimized and corroborated as a minimum on the corresponding potential energy surface at the r²SCAN-3c (CPCM (water)) level of theory. Colour code: C, grey; N, blue; O, red; H, white.

[7] F. Neese, *WIREs Comput. Mol. Sci.*, 2025, **15**, e70019.
[8] A. Blanco-Gómez, L. Barravecchia, E. Scarel, R. De Zorzi, L. Colomina-Alfaro, A. Bandiera, S. Kralj, A. Vila, D. Porrelli, C. Peinador, M. D. García and S. Marchesan, *ChemRxiv*, 2025, DOI: 10.26434/chemrxiv-2025-h4vwk.
[9] S. Grimme, A. Hansen, S. Ehlert and J.-M. Mewes, *J. Chem. Phys.*, 2021, **154**, 064103.
[10] V. Barone and M. Cossi, *J. Phys. Chem. A*, 1998, **102**, 1995.